Inorg. Chem. **2007**, *46*, 3057–3071

Syntheses, Crystal Structures, and Magnetic Properties of Metal–Organic Hybrid Materials of Cu(II): Effect of a Long Chain Dicarboxylate Backbone, and Counteranion in Their Structural Diversity

A. K. Ghosh,[†] D. Ghoshal,[‡] E. Zangrando,*[,§] J. Ribas,*[,||] and N. Ray Chaudhuri*[,†]

Department of Inorganic Chemistry, Indian Association for the Cultivation of Science, Kolkata-700 032, India, Department of Chemistry, Jadavpur University, Kolkata- 700 032, India, Dipartimento di Scienze Chimiche, University of Trieste, 34127 Trieste, Italy, and Departament de Química Inorgànica, Universitat de Barcelona, Diagonal 647, 08028- Barcelona, Spain

Received September 11, 2006

Eight new metal–organic hybrid materials of Cu(II) have been synthesized by using flexible glutarate/adipate as a bridging ligand, 2,2′-bipyridine/1,10-phenanthroline as a chelating ligand, and BF_4^-/ClO_4^-/Cl^- as a counteranion. These materials are characterized by single-crystal X-ray diffraction analyses and variable temperature magnetic measurements. Out of them, complexes **1**, **3**, **5**, and **8** crystallize in the triclinic system with space group $P\bar{1}$. Complexes **2**, **4**, **6**, and **7** crystallize in the monoclinic system with space group $P2_1/n$ (**2**, **4**), $P2_1/c$ (**6**), and $C2$ (**7**). The structural analysis reveals that bridging glutarate gives rise to dinuclear and tetranuclear species, whereas the adipate dianion leads to octanuclear, one-dimensional and two-dimensional polymeric complexes, although they have been prepared under similar conditions. Supramolecular architectures of higher dimensionality have been achieved through H-bonding and π–π interaction. In all the complexes, the bridging and/or counteranions as well as chelating ligand have a vital role in directing the solid-state structure. A variable temperature (2–300 K) magnetic susceptibility study discloses the antiferromagnetic coupling for all of the complexes.

Introduction

A tidal flow in the expressive research on crystal engineering[1] and supramolecular chemistry[2] has been put forward in the past decade because of the exploitation of rational design of metal−organic hybrid complexes via self-assembly[3] of metal ions and various multifunctional ligands. Along with common synthetic strategies, directed synthesis of self-assembly, with suitable anion and anion templation effects on self-assembly, has been successfully used and is among the most effective tools for synthesis.[4−7] It is evident that anions not only function in balancing the charge in metal−organic hybrid species, but they also play a crucial role in

* To whom correspondence should be addressed. E-mail: icnrc@iacs.res.in. Fax: 91-33-2473 2805 (N.R.C.), E-mail: ezangrando@units.it (E.Z.), E-mail: joan.ribas@qi.ub.es (J.R.).

[†] Indian Association of the Cultivation of Science.

[‡] Jadavpur University.

[§] University of Trieste.

[||] Universitat de Barcelona.

(1) (a) Braga, D.; Grepioni, F.; Orpen, A. G. In *Crystal Engineering: From Molecules, Crystals to Materials*; NATO Science Series, Mathematical and Physical Sciences, Vol. 538; Kluwer Academic Publishers: Dordrecht, The Netherlands, 1999. (b) Seddon, R. K.; Zaworotko, M. J. In *Crystal Engineering: The Design and, Application of Functional Solids*; NATO Science Series, Mathematical and Physical Sciences, Vol. 539, Kluwer Academic Publishers: Dordrecht, The Netherlands, 1999. (c) Desiraju, G. R. *Crystal Engineering: The Design of Organic Solids*; Elsevier Science Publishers B.V.: Amsterdam, The Netherlands, 1989.

(2) (a) Lehn, J.-M. *Supramolecular Chemistry−Concepts and Perspectives*; VCH: Weinheim, Germany, 1995. (b) Fujita, M. *Molecular Self-Assembly: Organic versus Inorganic Approaches; Structure and Bonding*, Vol. 96, Springer−Verlag: Berlin Heidelberg, Germany, 2000. (c) Atwood, J. L.; Steed, J. W. *Supramolecular Chemistry*; VCH: Verlag Gmbh, Weinheim, Germany, 2000. (d) Desiraju, G. R. In *The Crystals as a Supramolecular Entity*; Lehn, J. M. Ed.; John Wiley & Sons, Chester, U.K., 1996; Vol 2. (e) Desiraju, G. R. *Angew. Chem., Int. Ed. Engl.* **1995**, *34*, 2311.

(3) (a) Chin, D. N.; Zerkowski, J. A.; MacDonald, J. C.; Whitesides, G. M. *Organized Molecular Assemblies in the Solid State*; John Wiley and Sons: New York, 1999; pp 185−253. (b) Fujita, M. *Molecular Self-Assembly: Organic vs Inorganic Approaches;* Structure and Bonding, Vol. 96, Springer-Verlag: Berlin Heidelberg, Germany, 2000.

(4) (a) *Supramolecular Chemistry of Anions*, Bianchi, A., Bowman- James, K., Garcia-España, E., Eds.; Wiley-VCH: New York, 1997. (b) Berg, J. M. *Acc. Chem. Res.* **1995**, *28*, 14. (c) Beer, P. D.; Gale, P. A. *Angew. Chem., Int. Ed.* **2001**, *40*, 486.

(5) (a) Müller, A.; Das, S. K.; Bögge, H.; Beugholt, C.; Schmidtmann, M. *Chem. Commun.* **1999**, 1035. (b) Sánchez-Quesada, J.; Seel, C.; Prados, P.; de Mendoza, J. *J. Am. Chem. Soc.* **1996**, *118*, 277.

10.1021/ic061720v CCC: $37.00
Published on Web 03/21/2007

deriving structural diversity, such as to form bridges, helical structures, higher dimensional networks, etc. For example, a chloride anion acts generally as a bridging ligand,[8a,b] but sometimes it is organized in a cluster;[8c] planar anions (D_{3h}) such as NO_3^- and CO_3^{2-} originate two-dimensional (2D) and cyclic arrangements, respectively,[9] and tetrahedral (*Td*) ones, BF_4^- and ClO_4^-, play a key role in generating three-dimensional (3D) networks.[10] Anions such as N_3^-, SCN^-, dicyanamide, enolates, etc. have a tested efficiency in constructing a variety of networks as well as in participating in the spin exchange processes of transition metal complexes.[11−14] On the other hand, long chain dicarboxylates are excellent structure directing anions due to their flexible bridging capability for the construction of such metal−organic networks.[15,16] We have already studied the role of the succinate anion in the formation of solid-state structure,[16a] but the use of dicarboxylate glutarate[17−19] and adipate dianion[8c,20−22] can sustain more attractive discrete and infinite features. For the glutarate dianion, the aliphatic carbon backbone may be present in three conformations: anti−anti, anti−gauche, and gauche−gauche (Scheme 1).

Scheme 1

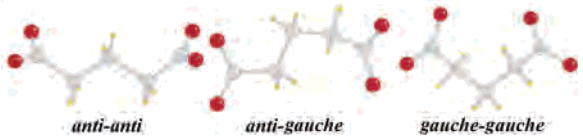

Of these the anti−anti and anti−gauche ones tend to be preferred in coordination compounds.[17a] However, the carbon chain of adipate is more flexible because the ligand may assume different conformations.[8c,20−22] These arrangements, along with the various orientations exhibited by the carboxylate group (with respect to the aliphatic chain), allow it to coordinate with transitional metal centers in different fashions. Moreover, these anions are capable of forming hydrogen bonds that yield higher dimensional structural motifs as well as porous structures. Researchers have recently exploited the combined effect of dicarboxylate bridging ligands and counteranions with aromatic N,N-donor chelating ligands that play a vital role in designing solid-state supramolecular architectures through $\pi-\pi$ stacking interactions[8c,14,16] and in controlling the metal−organic hybrid properties. The choice of planar N,N-donor chelating aromatic ligands is crucial because the presence of these synthons hampers the expansion of polymeric frameworks due to the "passivation" of the metal sites occupied by this ligand.

Knowing these properties, we have synthesized some new complexes of Cu(II) using glutarate (L) or adipate (L_1) as a bridging unit, 2,2′-bipyridine (bpy)/1,10-phenanthroline (phen) as a chelating ligand, and $BF_4^-/ClO_4^-/Cl^-$ as a counteranion. These complexes are of different nuclearity and dimensionality. We describe the synthesis and X-ray structural characterization of three new glutarato-bridged complexes of Cu(II) $[Cu(bpy)(L)(H_2O)]_2\cdot(H_3BO_3)_2\cdot(H_2O)_4$ (**1**), $[Cu_4(bpy)_4(L)_2(H_2O)_4](ClO_4)_4$ (**2**), and $[Cu_4(phen)_4(L)_2(H_2O)_2(ClO_4)_2](ClO_4)_2$ (**3**). Five adipato-bridged ones, namely $[Cu_8(phen)_{12}(L_1)_4](BF_4)_8\cdot(H_2O)_2$ (**4**), $\{[Cu(bpy)(L_1)(H_2O)]\cdot(H_2O)\}_n$ (**5**), $\{[Cu_2(bpy)_2(L_1)](ClO_4)_2\cdot(H_2O)_2\}_n$ (**6**), $\{[Cu_2(bpy)_2(L_1)(L_1H)](BF_4)\cdot(H_2O)_3\}_n$ (**7**), and $\{[Cu_4(phen)_4(L_1)_3](ClO_4)_2\cdot(H_2O)\}_n$ (**8**), are prepared under similar experimental conditions. Variable temperature magnetic susceptibility studies reveal antiferromagnetic coupling in all of them.

(6) (a) Fujita, M.; Nagao, S.; Ogura, K. *J. Am. Chem. Soc.* **1995**, *117*, 1649. (b) Fyfe, M. C. T.; Glink, P. T.; Menzer, S.; Stoddart, J. F.; White, A. J. P.; Williams, D. J. *Angew. Chem., Int. Ed. Engl*. **1997**, *36*, 2068. (c) Kim, Y. H.; Calabrese, J.; McEwen, C. *J. Am. Chem. Soc.* **1996**, *118*, 1545.

(7) (a) Alcalde, E.; Ramos, S.; Pérez-Garcia L. *Org. Lett.* **1999**, *1*, 1035. (b) Hasenknopf, B.; Lehn, J.-M.; Kneisel, B. O.; Baum, G.; D. Fenske, *Angew. Chem., Int. Ed. Engl.* **1996**, *35*, 1838. (c) Hasenknopf, B.; Lehn, J.-M.; Boumediene, N.; Dupont-Gervais, A.; Van Dorsselaer, A.; Kneisel, B.; Fenske, D. *J. Am. Chem. Soc.* **1997**, *119*, 10956.

(8) (a) Tabares, L. C.; Navarro, J. A. R.; Salas, J. M. *J. Am. Chem. Soc.* **2001**, *123*, 383. (b) Salta, J.; Chen, Q.; Chang, Y.; Zubieta, J. *Angew. Chem. Int. Ed. Engl.* **1994**, *33*, 757. (c) Ghosh, A. K.; Ghoshal, D.; Mostafa, G.; Ribas, J.; Ray Chaudhuri, N. *Cryst. Growth Des.* **2006**, *6*, 36.

(9) (a) Zhao, Y.-J.; Hong, M.-C.; Liang, Y.-C.; Su, W.-P.; Cao, R.; Zhou, Z.-Y.; Chan, A. S. C. *Polyhedron* **2001**, *20*, 2619. (b) Rarig, R. S.; Zubieta, J. *Inorg. Chim. Acta* **2001**, *319*, 235. (c) Fujita, M.; Kwon, Y. J.; Washizu, S.; Ogura, K. *J. Am. Chem. Soc.* **1994**, *116*, 1151. (d) Suen, M.-C.; Tseng, G.-W.; Chen, J.-D.; Keng, T.-C.; Wang, J.-C. *Chem. Commun.* **1999**, 1185.

(10) (a) Blake, A. J.; Champness, N. R.; Chung, S. S. M.; Li, W. -S.; Schröder, M. *Chem. Commun.* **1997**, 1675. (b) Jin, K.; Huang, X.; Pang, L.; Li, J.; Appel, A.; Wherland, S. *Chem. Commun.* **2002**, 2872. (c) Su, C. -Y.; Cai, Y. -P.; Chen, C. -L.; Lissner, F.; Kang, B. -S.; Kaim, W. *Angew. Chem., Int. Ed.* **2002**, *41*, 3371. (d) Sui, B.; Fan, J.; Okamura, T. A.; Sun, W. Y.; Ueyama, N. *New J. Chem.* **2001**, *25*, 1379.

(11) (a) Ribas, J.; Escuer, A.; Monfort, M.; Vicente, R.; Cortes, R.; Lezama, L.; Rojo, T. *Coord. Chem. Rev.* **1999**, *193*, 1027. (b) Ghosh, A. K.; Ghoshal, D.; Zangrando, E.; Ribas, J.; Ray Chaudhuri, N. *Inorg. Chem.* **2005**, *44*, 1786.

(12) (a) Zhang, H.; Wang, X.; Zhang, K.; Teo, B. K. *Coord. Chem. Rev.* **1999**, *183*, 157. (b) Golub, A. M.; Kohler, H.; Skepenko, V. V. *Chemistry of Pseudohalides*; Elsevier: Amsterdam, 1986.

(13) (a) Batten, S. R.; Murray, K. S. *Coord. Chem. Rev.* **2003**, *246*, 103. (b) Ghoshal, D. Ghosh, A. K.; Ribas, J.; Zangrando, E.; Mostafa, G.; Maji, T. K.; Ray Chaudhuri, N. *Cryst. Growth Des.* **2005**, *5*, 941.

(14) (a) Yaghi, O. M.; Li, G.; Groy, T. L. *J. Chem. Soc. Dalton Trans.* **1995**, 727. (b) Ghoshal, D.; Ghosh, A. K.; Ribas, J.; Mostafa, G.; Ray Chaudhuri, N. *CrystEngComm.* **2005**, *7*, 616. (c) Ghosh, A. K.; Ghoshal, D.; Zangrando, E.; Ribas, J.; Ray Chaudhuri, N. *Dalton Trans.* **2006**, 1554.

(15) (a) Hornick, C.; Rabu, P.; Drillon, M. *Polyhedron* **2000**, *19*, *259*. (b) Bowden, T. A.; Milton, H. L.; Slawin, A. M. Z.; Lightfoot, P. *Dalton Trans.* **2003**, 936. (c) Bazzicalupi, C.; Bencini, A.; Bianchi, A.; Fusi, V.; España, E. G.; Giorgi, C.; Llinares, J. M.; Ramirez, J. A.; Valtancoli, B. *Inorg. Chem.* **1999**, *38*, 620.

(16) (a) Ghoshal, D.; Maji, T. K.; Mostafa, G.; Sain, S.; Lu, T. -H.; Ribas, J.; Zangrando, E.; Ray Chaudhuri, N.; *Dalton Trans.* **2004**, 1687. (b) Ghosh, A. K.; Jana, A. D.; Ghoshal, D.; Mostafa, G.; Ray Chaudhuri, N. *Cryst. Growth Des.* **2006**, *6*, 701. (c) Frisch, M.; Cahill, C. L. *Dalton Trans*. **2005**, 1518.

(17) (a) Rather, B.; Zaworotko, M. J. *Chem. Commun.* **2003**, 830. (b) Lee, E. W.; Kim, Y. J.; Jung, D.-Y. *Inorg. Chem.* **2002**, *41*, 501. (c) Kim, Y. J.; Park, Y. J.; Jung, D.-Y. *Dalton Trans.* **2005**, 2603.

(18) (a) Guillou, N.; Livage, C.; Drillon, M.; Férey, G. *Angew. Chem., Int. Ed.* **2003**, *42*, 5314. (b) Vaidhyanathan, R.; Natarajan, S.; Rao, C. N. R. *J. Solid State Chem.* **2004**, *177*, 1444.

(19) (a) Kim, J.-S.; Kim, H.; Ree, M. *Chem. Mater.* **2004**, *16*, 2981. (b) Serpaggib, F.; Férey, G. *J. Mol. Struct.* **2003**, *656*, 201.

(20) (a) Mukherjee, P. S.; Konar, S.; Zangrando, E.; Mallah, T.; Ribas, J.; Ray Chaudhuri, N. *Inorg. Chem.* **2003**, *42*, 2695. (b) Kim, Y. J.; Jung, D.-Y. *Inorg. Chem.* **2000**, *39*, 1470. (c) Hao, N.; Shen, E.; Li, Y.-G.; Wang, E.-B.; Hu, C.-W.; Xu, L. *Eur. J. Inorg. Chem.* **2004**, 4102.

(21) (a) Ying, E.-B.; Zheng, Y.-Q.; Zhanga, H.-J. *J. Mol. Struct.* **2004**, *693*, 73. (b) Kim, Y. J.; Suh, M.; Jung, D.-Y. *Inorg. Chem.* **2004**, *43*, 245. (c) de Lill, D. T.; Gunning, N. S.; Cahill, C. L. *Inorg. Chem.* **2005**, *44*, 258.

(22) (a) Kurmoo, M. *J. Mater. Chem.* **1999**, *9*, 2595. (b) Sieroń, L.; Bukowska-Strzyżewska, M.; Korabik, M.; Mroziński J. *Polyhedron* **2002**, *21*, 2473.

Experimental Section

Materials. High purity Cu(II) chloride dihydrate and Cu(II) tetrafluoroborate hydrate were purchased from Aldrich Chemical Co. Inc. and used as received. All other chemicals were of AR grade.

Physical Measurements. Elemental analyses (carbon, hydrogen, and nitrogen) were performed using a Perkin-Elmer 240C elemental analyzer. IR spectra were measured from KBr pellets on a Nicolet 520 Fourier transform IR (FTIR) spectrometer. The magnetic measurements were carried out in the "Servei de Magnetoquímica (Universitat de Barcelona)" on polycrystalline samples (30 mg) with a Quantum Design superconducting quantum interference device (SQUID) MPMS-XL magnetometer working in the 2−300 K range. The magnetic field was 0.1 T. The diamagnetic corrections were evaluated from Pascal's constants.[23]

Synthesis of 1. On addition of an aqueous solution (10 mL) of disodium glutarate (0.162 g, 1 mmol) to a methanolic solution (5 mL) of Cu(II) tetrafluoroborate hydrate, (0.237 g, 1 mmol) a sky-blue compound was separated out. A methanolic solution (5 mL) of 2,2′-bipyridine (0.156 g, 1 mmol) was added to it and the sample was refluxed for 4 h. The deep-blue solution derived after filtration was stored in a calcium chloride desiccator. Deep-blue, shiny single crystals suitable for X-ray analysis were obtained following one week of storage. Yield was 75%. Anal. Calcd. for $C_{30}H_{46}B_2Cu_2N_4O_{20}$: C, 38.65; H, 4.94; N, 6.01 (%). Found: C, 38.53; H, 4.78; N, 5.91 (%). IR (KBr, cm^{-1}) 3439 (ν_{OH}); 2929−2858 (ν_{CH}); 1602, 1558, and 1541 (ν_{as}OCO); 1449 and 1394 (ν_sOCO); 1275 ($\delta_{C=O}$); 784 (νH_3BO_3); 737 and 661 (ρ_rH_2O); 533 (ρ_wH_2O).

All of the other complexes were synthesized by a similar procedure adopted for complex **1** but using the appropriate reagents as indicated.

Synthesis of 2. Copper(II) perchlorate hexahydrate (0.370 g, 1 mmol) was used instead of Cu(II) tetrafluoroborate hydrate. Deep-blue, block-shaped single crystals of **2,** suitable for X-ray diffraction, were obtained following a week of storage. Yield was 72%. Anal. Calcd. for $C_{50}H_{52}Cl_4Cu_4N_8O_{28}$: C, 37.29; H, 3.23; N, 6.96 (%). Found: C, 37.18; H, 3.19; N, 6.79 (%). IR (KBr, cm^{-1}) 3542−3078 (ν_{OH}); 2945 (ν_{CH}); 1718, 1603, 1521, and 1506 (ν_{as}OCO); and 1480, 1445, 1415, and 1315 (ν_sOCO); 1252 ($\delta_{C=O}$); 1091-(νClO); 772 and 731 (ρ_rH_2O); 628 (ρ_wH_2O).

Synthesis of 3. Copper(II) perchlorate hexahydrate (0.370 g, 1 mmol) was used in place of Cu(II) tetrafluoroborate hydrate and 1,10-phenanthroline (0.198 g, 1 mmol) was used instead of 2,2′-bipyridine. Suitable single crystals of **3** for X-ray analysis were obtained following two weeks of storage. Yield was 68%. Anal. Calcd. for $C_{29}H_{24}Cl_2Cu_2N_4O_{13}$: C, 41.70; H, 2.87; N, 6.71 (%). Found: C, 41.67; H, 2.76; N, 6.68 (%). IR (KBr, cm^{-1}) 3502−3005 (ν_{OH}); 2958−2872 (ν_{CH}); 1579 and 1515 (ν_{as}OCO); 1457, 1421, and 1342 (ν_sOCO); 1290 and 1228 ($\delta_{C=O}$); 1161−1086 (νClO); 846 and 720 (ρ_rH_2O); 629, 677, and 551(ρ_wH_2O).

Synthesis of 4. 1,10-Phenanthroline (0.198 g, 1 mmol) was used in place of 2,2′-bipyridine, and disodium adipate (0.190 g, 1 mmol) was used instead of disodium glutarate. Single crystals of **4**, suitable for X-ray diffraction, were obtained following two weeks of storage. Yield was 67%. Anal. Calcd. for $C_{168}H_{132}B_8Cu_8F_{32}N_{24}O_{18}$: C, 50.68; H, 3.32; N, 8.45 (%). Found: C, 50.61; H, 3.29; N, 8.41 (%). IR (KBr, cm^{-1}) 3436−3058 (ν_{OH}); 2929−2859 (ν_{CH}); 1587, 1548, and 1526 (ν_{as}OCO); 1460 and 1428 ν_s(OCO); 1083 and 1062 (ν_{ClO}); 850 and 722 (ρ_rH_2O); 650, 526, and 426 (ρ_wH_2O).

Synthesis of 5. Copper(II) chloride dihydrate (0.170 g, 1 mmol) and disodium adipate (0.190 g, 1 mmol) were used in place of Cu(II) tetrafluoroborate hydrate and of disodium glutarate, respectively. Single crystals of **5**, suitable for X-ray diffraction, were obtained after a few days of storage. Yield was 77%. Anal. Calcd. for $C_{16}H_{20}CuN_2O_6$: C, 48.01; H, 5.00; N, 7.00 (%). Found: C, 47.69; H, 4.91; N, 6.78 (%). IR (KBr, cm^{-1}) 3528−3436 (ν_{OH}); 2960−2868 (ν_{CH}); 1560 (ν_{as}OCO); 1417, 1396, and 1320 (ν_sOCO); 1224 ($\delta_{C=O}$); 794 (ρ_rH_2O); 661 and 625 (ρ_wH_2O).

Synthesis of 6. Copper(II) perchlorate hexahydrate (0.370 g, 1 mmol) was used in place of Cu(II) tetrafluoroborate hydrate, and disodium adipate (0.190 g, 1 mmol) was used instead of disodium glutarate. Single crystals of **6**, suitable for X-ray diffraction, were obtained following one week of storage. Yield was 73%. Anal. Calcd. for $C_{26}H_{28}Cl_2Cu_2N_4O_{14}$: C, 38.12; H, 3.42; N, 6.84 (%). Found: C, 38.09; H, 3.38; N, 6.79 (%). IR (KBr, cm^{-1}) 3432−3118 (ν_{OH}); 2932−2866 (ν_{CH}); 1582 (ν_{as}OCO); 1444, 1411, and 1312 (ν_sOCO); 1143, 1115, and 1086 (ν_{ClO}); 772 and 738 (ρ_rH_2O); 678 and 628 (ρ_wH_2O).

Synthesis of 7. Disodium adipate (0.190 g, 1 mmol) was used in place of disodium glutarate. Deep-blue, single crystals of **7**, suitable for X-ray diffraction, were obtained following a few weeks of storage. Yield was 61%. Anal. Calcd. for $C_{32}H_{39}BCu_2F_4N_4O_{11}$: C, 44.16; H, 4.48; N, 6.44 (%). Found: C, 44.09; H, 4.41; N, 6.42 (%). IR (KBr, cm^{-1}) 3426−3068 (ν_{OH}); 2932−2860 (ν_{CH}); 1602 and 1573 (ν_{as}OCO); 1448, 1416, and 1319 (ν_sOCO); 1079−969 (ν_{BF})]; 897, 871, 773, and 728 (ρ_rH_2O); 671 and 557 (ρ_wH_2O).

Synthesis of 8. Copper(II) perchlorate hexahydrate (0.370 g, 1 mmol), 1,10-phenanthroline (0.198 g, 1 mmol), and disodium adipate (0.190 g, 1 mmol) were used instead of Cu(II) tetrafluoroborate hydrate, 2,2′-bipyridine, and disodium glutarate, respectively. Deep-blue, single crystals of **8**, suitable for X-ray analysis, were obtained following a few weeks of storage. Yield was 70%. Anal. Calcd. for $C_{66}H_{58}Cl_2Cu_4N_8O_{21}$: C, 48.76; H, 3.57; N, 6.89 (%). Found: C, 48.71; H, 3.51; N, 6.82 (%). IR (KBr, cm^{-1}) 3469−3085 (ν_{OH}); 2952−2866 (ν_{CH}); 1613, 1552, and 1520 (ν_{as}OCO); 1428, 1367, and 1334 (ν_sOCO); 1215, 1155, and 1094 (ν_{ClO}); 877, 864, 784, 751, and 731 (ρ_rH_2O); 651 (ρ_wH_2O).

Crystallographic Data Collection and Refinement. Crystal data of the structures reported are summarized in Tables 1 and 2. Diffraction data for complexes **6** and **8** were carried out on a Nonius DIP-1030H system with Mo−Kα radiation (λ = 0.71073 Å), and those for **7** on an Enraf-Nonius rotating anode (Cu−Kα, λ= 1.54178 Å) equipped with a Kappa CCD detector. Cell refinement, indexing, and scaling were performed using the programs Mosflm,[24] Denzo,[25] and Scalepack.[25] All of the structures were solved by direct methods and subsequent Fourier analyses,[26] and refinement was performed by the full matrix least-squares method based on F^2 with all observed reflections.[26] The choice of the noncentrosymmetric space group *C*2 for **7** was confirmed by the successful final refinement; however, the Flack parameter, 0.47(3), indicates a racemic twinning of the crystal. In **2** a ClO_4^- anion was found to be disordered over two positions, with 0.5 occupancy each. The phenanthroline carbon atoms of **4** were isotropically refined for the low number of observed reflections ($I > 2\sigma(I)$), as well as for fluorines at lower occupancy of a disordered BF_4^- anion. Hydrogen atoms were placed at their geometrical positions, and those of water molecules (except for lattice molecules of **4** and **8**) were located

(23) Kahn, O. *Molecular Magnetism*, VCH: Weinheim, Germany, 1993.

(24) *Collaborative Computational Project*, Number 4, *Acta Crystallogr.* **1994**, *D50*, 760.

(25) Otwinowski, Z.; Minor, W. In *Processing of X-ray Diffraction Data Collected in Oscillation Mode*, Carter, C. W. Jr., Sweet, R. M., Eds.; *Methods in Enzymology, Macromolecular Crystallography*, part A; Academic Press: New York, 1997; Vol. 276, pp 307−326.

(26) SHELX97. Sheldrick, G. M. Institüt für Anorganische Chemie der Universität, Tammanstrasse 4, D-3400 Göttingen, Germany, 1998.

Table 1. Crystallographic Data for Complexes **1**−**4**

	1	**2**	**3**	**4**
empirical formula	$C_{30}H_{46}B_2Cu_2N_4O_{20}$	$C_{50}H_{52}Cl_4Cu_4N_8O_{28}$	$C_{29}H_{24}Cl_2Cu_2N_4O_{13}$	$C_{168}H_{132}B_8Cu_8F_{32}N_{24}O_{18}$
fw	931.41	1608.96	834.50	3977.78
cryst system	triclinic	monoclinic	triclinic	monoclinic
space group	$P\bar{1}$	$P2_1/n$	$P\bar{1}$	$P2_1/n$
a, Å	8.748(2)	9.224(3)	10.619(3)	19.313(4)
b, Å	10.528(2)	18.761(4)	11.937(2)	12.849(4)
c, Å	12.232(3)	18.889(4)	14.120(3)	34.762(6)
α, deg	101.13(2)		79.52(2)	
β, deg	94.29(2)	103.87(2)	77.65(2)	90.94(2)
γ, deg	111.49(2)		66.99(3)	
V, Å^3	1015.4(4)	3173.5(14)	1599.7(6)	8625(4)
Z	1	2	2	2
D_{calcd} g·cm^{-3}	1.523	1.684	1.733	1.532
μ (Mo−Kα), mm^{-1}	1.130	1.582	1.571	1.072
F(000)	482	1632	844	4024
range, deg	2.14−29.65	2.22−26.37	2.38−26.37	1.90−22.46
no. of reflns collcd	12 195	28 948	17 674	58 047
no. of indep reflns	5207	6147	6001	10972
R_{int}	0.0310	0.0539	0.0643	0.1147
no. of reflns $I > 2\sigma(I)$	4182	3829	3711	5155
no. of refined params	289	433	457	794
goodness-of-fit (F^2)	1.002	0.913	1.041	0.901
*R*1 ($I > 2\sigma(I)$)[a]	0.0381	0.0478	0.0636	0.0737
*wR*2[a]	0.1066	0.1288	0.1604	0.2000
residuals, e/Å^3	0.342, −0.268	0.537, −0.595	0.663, −0.790	0.882, −0.473

[a] $R1 = \sum||Fo| - |Fc||/\sum|Fo|$, $wR2 = [\sum w(Fo^2 - Fc^2)^2/\sum w(Fo^2)^2]^{1/2}$.

Table 2. Crystallographic Data for Complexes **5**−**8**

	5	**6**	**7**	**8**
empirical formula	$C_{16}H_{20}CuN_2O_6$	$C_{26}H_{28}Cl_2Cu_2N_4O_{14}$	$C_{32}H_{39}BCu_2F_4N_4O_{11}$	$C_{66}H_{58}Cl_2Cu_4N_8O_{21}$
fw	399.88	818.50	869.56	1624.26
cryst system	triclinic	monoclinic	monoclinic	triclinic
space group	$P\bar{1}$	$P2_1/c$	*C*2	$P\bar{1}$
a, Å	6.876(2)	15.010(3)	12.122(3)	13.198(3)
b, Å	10.482(3)	11.733(1)	14.368(3)	16.373(4)
c, Å	12.390(3)	18.454(3)	21.533(4)	18.340(5)
α, deg	85.40(3)			115.59(2)
β, deg	82.72(2)	95.374(2)	100.20(3)	98.70(2)
γ, deg	73.77(3)			101.80(3)
V, Å^3	849.6(4)	3235.7(9)	3691.1(14)	3367.7(15)
Z	2	4	4	2
D_{calcd}, g·cm^{-3}	1.563	1.680	1.565	1.602
μ (Mo−Kα), mm^{-1}	1.321	1.553	2.158	1.408
F(000)	414	1664	1784	1656
θ range, deg	2.03−29.67	2.06−28.29	5.93−64.77	1.28−25.03
no. of reflns collcd	11 936	20 436	23 083	34 176
no. of indep reflns	3977	7785	5273	11 067
R_{int}	0.0280	0.1363	0.0440	0.0546
no. of reflns $I > 2\sigma(I)$	2669	2025	4975	5713
no. of refined params	238	433	507	910
goodness-of-fit (F^2)	0.933	0.906	1.056	0.956
*R*1 ($I > 2\sigma(I)$)[a]	0.0413	0.0538	0.0564	0.0465
*wR*2[a]	0.1082	0.1266	0.1538	0.1044
residuals, e/Å^3	0.268, −0.353	0.651, −0.584	0.540, −0.318	0.573, −0.339

[a] $R1 = \sum||Fo| - |Fc||/\sum|Fo|$, $wR2 = [\sum w(Fo^2 - Fc^2)^2/\sum w(Fo^2)^2]^{1/2}$.

on a ΔFourier map by restraining the O−H distances. All calculations were performed using the WinGX System, Ver 1.64.[27]

Results and Discussion

Synthesis. During preparation of the complexes, we refluxed the mixture of the reactants [Cu(II) salt, disodium dicarboxylate, N,N-donor chelate] in equimolecular proportions. Elemental analysis of the derived complexes reveals that, in most of the cases, composition of the complexes does not corroborate with the reactants ratio used. With an aim to achieve an optimum ratio, any attempt to synthesize the complexes using arbitrary ratios of the reactants resulted in the formation of compounds having the same stoichiometry. However, it is important to note that the syntheses performed using the ratio of the reactants observed in derived complexes enhanced their yield to a measurable extent.

The tetrafluroborate anion remains intact in complexes **4** and **7** but gets hydrolyzed to boric acid[28] during preparation of complex **1**. In all cases glutarate/adipate exists as a dianion. Interestingly, in complex **7**,one of the two crystallographic adipate units is present as a monoanion. The

(27) Farrugia, L. J. *J. Appl. Crystallogr*. **1999**, *32*, 837.

(28) (a) Booth, H. S.; Martin, D. R. *Boron Trifluoride and Its Derivatives*; John Wiley & Sons, Inc.: New York, 1949. (b) Ruiss, I. G.; Bakina, N. P. *Compt. Rend. Acad. Sci. U.R.S.S. (N.S.)* **1936**, *2*, 107.

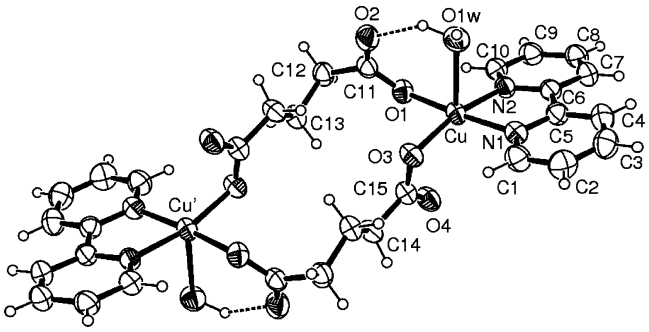

Figure 1. An ORTEP drawing of the dinuclear species of **1** with labeling scheme of the crystallographic independent unit.

Table 3. Coordination Bond Lengths (Å) for Glutarate Complexes **1**−**3**

	Complex **1**[a]		
Cu−O(1)	1.959(1)	Cu−N(1)	1.995(2)
Cu−O(3)	1.966(2)	Cu−N(2)	2.007(2)
Cu−O(1w)	2.388(2)	Cu−Cu′	8.144(2)
	Complex **2**[a]		
Cu(1)−O(1)	1.957(4)	Cu(2)−O(2)	1.959(3)
Cu(1)−O(3)	1.943(3)	Cu(2)−O(4)	1.952(4)
Cu(1)−N(1)	2.007(4)	Cu(2)−N(3)	2.007(4)
Cu(1)−N(2)	1.990(4)	Cu(2)−N(4)	1.999(5)
Cu(1)−O(1w)	2.225(4)	Cu(2)−O(2w)	2.212(4)
Cu(1)−Cu(2)	3.032(1)	Cu(1)−Cu(2′)	8.408(2)
	Complex **3**[a]		
Cu(1)−O(1)	1.951(5)	Cu(2)−O(2)	1.930(4)
Cu(1)−O(3)	1.938(4)	Cu(2)−O(4)	1.943(4)
Cu(1)−N(1)	2.031(6)	Cu(2)−N(3)	2.004(5)
Cu(1)−N(2)	1.991(5)	Cu(2)−N(4)	2.009(5)
Cu(1)−O(1w)	2.205(5)	Cu(2)−O(11)	2.438(6)
Cu(1)−Cu(2)	3.012(1)	Cu(1)−Cu(2′)	7.830(3)

[a] Symmetry code: (′) $1-x, -y, 1-z$.

crystals, isolated in the synthesis of **7** using adipic acid instead of disodium adipate, showed the absence of BF_4^- anions on analysis, but they were unsuitable for X-ray diffraction study. However, complex **7** also can be synthesized using partially neutralized adipic acid.

Structure Description of Complex 1. The crystal structure of **1** consists of dinuclear neutral $[Cu(bpy)(L)(H_2O)]_2$ five-coordinate Cu(II) units (Figure 1), boric acid, and lattice water molecules. The complex is located about an inversion center with the metals in a distorted square pyramidal coordination environment. The coordination bond lengths are reported in Table 3. The basal plane sites are occupied by bpy nitrogen donors [Cu−N(1) = 1.995(2) and Cu−N(2) = 2.007(2) Å], by two oxygens from different glutarate dianions [Cu−O(1) = 1.959(2) and Cu−O(3) = 1.966(2) Å], and an aquo ligand is located at the apical site at a significantly longer distance [Cu−O(1w) = 2.388(2) Å]. The copper ion is displaced by 0.11 Å from the basal N_2O_2 plane toward the fifth coordination site. The dicarboxylate dianions act in a bis-unidentate coordination mode and bridge the metals at 8.144(2) Å. The aqua ligand forms a strong intramolecular H-bond with the uncoordinated oxygen of the glutarate dianion [O(1w)−O(2) = 2.660(3) Å] and another interaction involving a lattice water molecule [O(1w)−O(3w) = 2.734(3) Å]. A 2D structure is built by an extended network of H-bonding (Table S1, Supporting information) among boric acid molecules, lattice water oxygens, and carboxylate

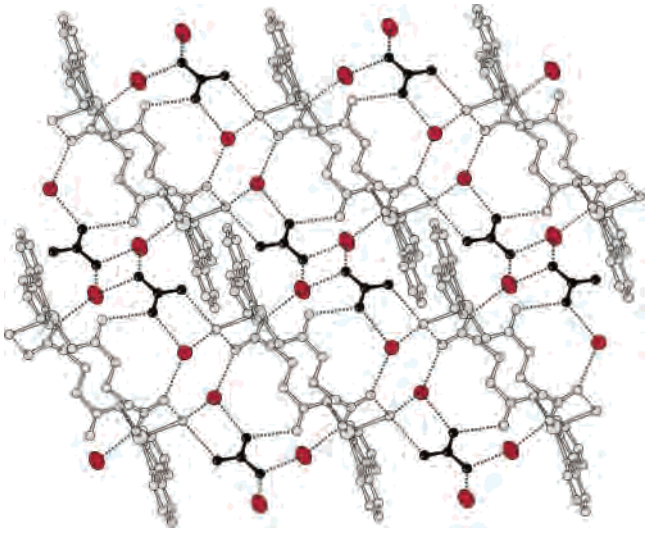

Figure 2. The H-bonding scheme forming a 2D architecture in **1** [where boric acid = black spheres and lattice water molecules = ellipses].

Table 4. Face-to-Face $\pi-\pi$ Interactions in Complexes **1**−**8**

complex/ *N,N′* ligand	ring(*i*)/ring(*j*)[a,b]	dihedral angle (i,j) deg	distance between centroids, Å
1/ bpy	N(2)/N(2a)	0.00	3.900
2/ bpy	N(1)/N(3)[c]	10.8(3)	3.755
	N(2)/N(4)[c]	7.0(3)	3.807
3/ phen	N(1)/N(3)[c]	7.3(4)	3.474
	N(2)/N(4)[c]	6.9(4)	3.590
	N(1)/N(1b)	0.00	3.700
	N(1)/R(1b)	1.06	3.764
4/ phen	N(3)/N(5)[c]	8.90	3.835
	N(5)/N(7c)[c]	10.34	3.701
	N(7)/N(9)[c]	8.02	3.796
	N(4)/N(6)[c]	6.71	3.989
	N(6)/N(8c)[c]	13.47	4.067
	N(8)/N(10)[c]	8.35	4.070
	N(11)/N(11a)	8.00	3.840
	N(11)/N(1a)	0.00	3.716
5/ bpy	N(1)/N(2d)	2.49	3.635
	N(1)/N(2e)	2.49	4.658
6/ bpy	N(1)/N(3)[c]	10.04	3.618
	N(2)/N(4)[c]	7.60	3.670
	N(1)/N(2f)	3.56	4.462
	N(2)/N(1f)	3.56	4.462
7/ bpy	N(1)/N(2g)	13.21	3.595
	N(3)/N(4h)	16.07	3.731
8/ phen	N(2)/N(2i)	0.00	3.670
	N(3)/N(8f)	16.07	4.135
	N(7)/N(7j)	0.00	3.972

[a] N(i) indicates a pyridine ring and R(1) = C4−C5-C6−C7-C21−C22. [b] Symmetry codes: (a) $1-x, 2-y, 1-z$; (b) $-x, -y, 2-z$; (c) $-x, 2-y, 1-z$; (d) $2-x, -y, 1-z$; (e) $1-x, -y, 1-z$; (f) $-x, -y, 1-z$; (g) $1-x, y, 1-z$; (h) $2-x, y, -z$; (i) $-x, 1-y, 2-z$; (j) $1-x, 1-y, 1-z$. [c] Indicates facing *N,N′* ligands between the bridged copper dimer.

groups (Figure 2), while a 3D architecture is achieved through $\pi-\pi$ bpy ligand interactions of stacking layers that occurs between symmetry related N(2) pyridine rings of an adjacent 2D unit (Table 4).

Structure Description of Complex 2. It is comprised of a tetranuclear $\{[Cu(bpy)(H_2O)]_4(L)_2\}^{4+}$ cationic species and perchlorate anions. Figure 3 depicts an Oak Ridge thermal ellipsoid plot (ORTEP) view of the complex located about a center of symmetry. The dicarboxylate dianion acts as a bis-bridging ligand toward the copper ions, Cu(1) and Cu(2), which are 3.032(1) Å apart, while the Cu(1)−Cu(2′)

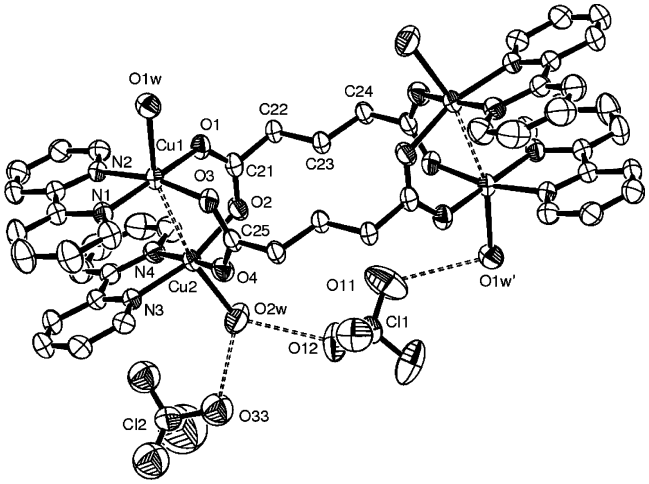

Figure 3. An ORTEP drawing of the centrosymmetric tetranuclear species of **2** with labeling scheme of relevant atoms.

distance separated by the glutarate is 8.408(2) Å. Both metals present a distorted square pyramidal coordination geometry through bpy nitrogen donors, two carboxylate oxygens, and an apical water molecule. The Cu−N bond lengths fall in a range of 1.990(4)−2.007(4) Å, slightly longer than the Cu−O bonds [1.943(3)−1.959(3) Å], while the apical Cu(1)−O(1w) and Cu(2)−O(2w) distances are 2.225(4) and 2.212(4) Å, respectively (Table 3). The atoms in the basal planes are coplanar (within ±0.08 Å) with Cu(1) and Cu(2) atoms displaced by 0.13 and 0.14 Å, respectively, toward the apical oxygen donor. In the dinuclear unit, the coordination planes form a dihedral angle of 22.64(1)°, and the angle formed by the bpy ligands is 8.9(2)°. The former value indicates that the basal planes are rather distorted due to the carboxylate bite angles, and the almost parallel angle delineated by the bpy planes shows a strong intramolecular $\pi-\pi$ interaction. On the other hand, no $\pi-\pi$ interaction involving aromatic rings of different complex units is observed. The water molecules form H-bonds with perchlorate oxygens (O−O distances of 2.79−2.97 Å), as indicated in the lower part of Figure 3. These interactions provide a justification of the non-collinear Cu−Cu−OH_2 fragments (ca 162.7°) and the disorder found in the Cl(2) perchlorate anion (two orientations, each with 50% occupancy) is likely caused to favor the formation of H-bonds. The result is a 2D undulated network, as depicted in Figure 4, but no $\pi-\pi$ interaction is operative between them.

Structure Description of Complex 3. It consists of a tetranuclear $[Cu_2(phen)_2(H_2O)(ClO_4)]_2(L)_2^{2+}$ species and perchlorate anions. Figure 5 shows an ORTEP view of the metal complex that is structurally similar to the cation of complex **2** by replacing the chelating bpy with phen ligands and an aqua ligand (and its symmetry related one) by a ClO_4^- anion. In fact, the coordination bond distances (Table 3) and angles indicate close, comparable values with those of **2**. The only exception is represented by the apical Cu−O(11) bond length involving a perchlorate oxygen, 2.438(6) Å, which is significantly longer than the Cu(1)−O(1w) bond length, 2.205(5) Å. The axial Cu(2)−Cu(1)−O(1w) fragment is almost linear [175.33(14)°], while the value observed for Cu-

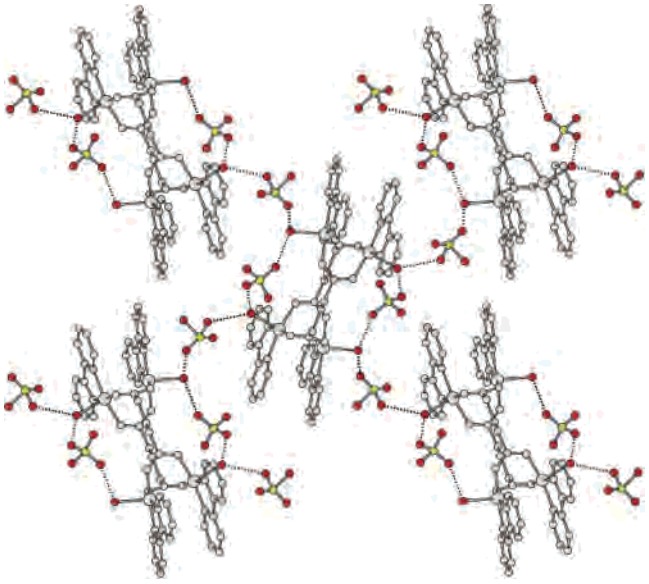

Figure 4. A 2D layer projected on the *bc*-plane showing H-bonds among water ligands and ClO_4^- in **2**.

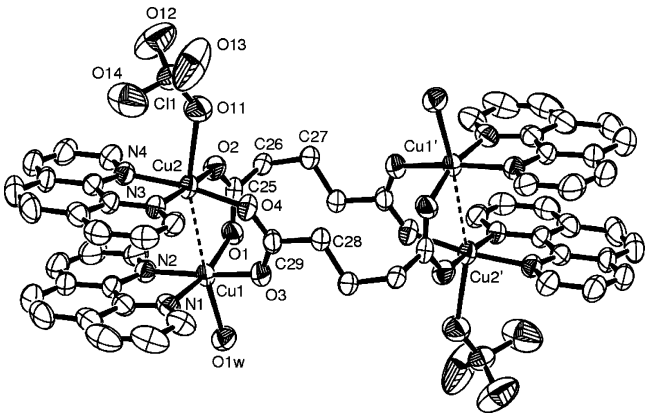

Figure 5. An ORTEP drawing of the centrosymmetric tetranuclear species of **3** with the labeling scheme of relevant atoms.

(1)−Cu(2)−O(11) [161.73(14)°] may be caused by the steric hindrance of the ClO_4^- anion. The Cu(1)−Cu(2) distance, between copper ions bearing $\pi-\pi$ interacting phen ligands, is 3.012(1) Å, and the Cu(1)−Cu(2′) distance connected by the bis-bridging glutarate is 7.830(3) Å. The donors in the basal plane are almost coplanar, ±0.058 and 0.036 Å for the coordination sphere of Cu(1) and Cu(2) ions, respectively, and each metal is slightly displaced from its plane toward the apical ligand donor by 0.18 and 0.07 Å, respectively. The coordination planes make a dihedral angle of 22.7(21)°, and the angle formed by the $\pi-\pi$ interacting phen ligands is 6.8(2)°, which indicates a conformational distortion very similar to that found in **2**. The crystal packing shows tetranuclear complexes connected through H-bonds occurring between aquo ligands and perchlorate anions [O−O distances of 2.848(8) and 2.855(9) Å] forming a one-dimensional (1D) polymeric arrangement (Figure 6). The adjacent 1D chains interdigitate to form face-to-face $\pi-\pi$ interactions between the phen N(1) pyridine ring with a symmetry related one, giving rise to a 2D supramolecular network.

Structural Comparison of Glutarate Complexes. A detailed analysis of coordination geometrical data for glut-

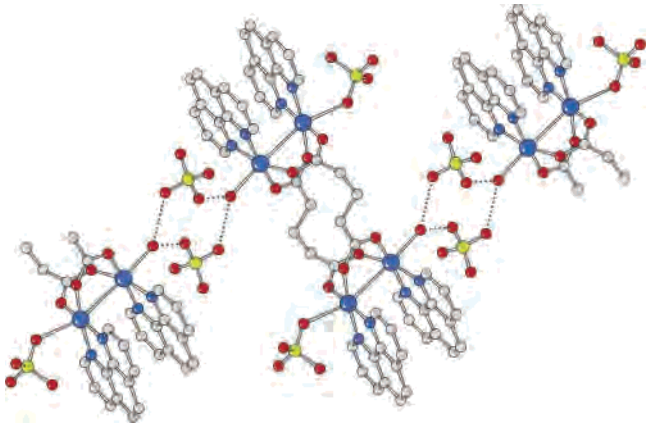

Figure 6. Tetranuclear units connected through H-bonds in **3**.

arate containing complexes indicates close, comparable Cu−N bond distances, varying from 1.990(4) to 2.031(6) Å, regardless of the presence of a bpy/phen ligand, as well as Cu−O(glutarate) distances that fall in a narrow range of 1.930(4)−1.966(2) Å. More significant differences are displayed by the apical Cu−O distances. In fact the Cu−O(1w) bond length in **1** [2.388(2) Å] is longer than the Cu−O(aquo) distances in **2** and **3** that average 2.214(4) Å. These features may be explained by considering that the aquo ligand in **1** is involved in strong H-bonds and in the other complexes the axial water molecules weakly interact as an H-donor toward ClO_4^- anions. The Cu−O(perchlorate) distance observed in **3** is 2.438(6) Å, which is the longest among the apical Cu−O distances for steric effects. It is noteworthy that the conformation adopted by the glutarate chains modulates the metal−metal distance inside these centrosymmetric complexes. In fact, complexes **1** and **3**, which have a twisted carbon aliphatic backbone of glutarate dianion [torsion angles of 65.6(2) and 169.98(17)° and of 75.1(5) and 180.0(6)°, respectively] show a Cu−Cu distance of 8.144(2) and 7.830(3) Å. These intermetallic distances are significantly shorter with respect to the values 8.408(2) Å observed in **2** and 8.467 Å reported for the $[Cu(phen)(H_2O)(L)]_2$ complex,[29] which is structurally similar to **1** but contains phen instead of bpy as the ligand. In the latter structures the dianion shows an extended chain (anti−anti conformation).

Structure Description of Complex 4. The crystal structure determination reveals an octanuclear cationic $[Cu_8(phen)_{12}(L_1)_4]^{8+}$ entity, arranged on an inversion center, and similar to the succinate derivative recently reported by this laboratory.[16a] As already suggested, the BF_4^- counteranion seems to favor the formation of this cluster, thereby disrupting the expected supramolecular 1D/2D motif with the appearance of edge-to-face interactions between phen chelating ligands. An ORTEP drawing of the complex **4** is shown in Figure 7, and a selection of bond distances is reported in Table 5. The coordination around each copper ion is approximately square pyramidal. The basal sites for the lateral Cu(1) and Cu(4) ions are occupied by three N donors of chelating phen and oxygens O(1) and O(8) of the

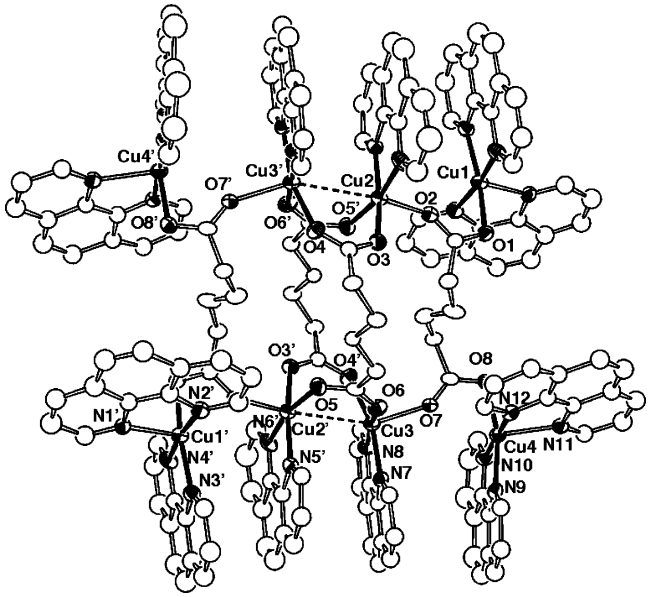

Figure 7. An ORTEP drawing of the octanuclear cation of **4** also with the labeling scheme of ligand donor atoms.

Table 5. Coordination Bond Lengths (Å) for Complex **4**[a]

Cu(1)−O(1)	1.979(7)	Cu(2)−O(3)	1.935(7)
Cu(1)−N(2)	2.031(10)	Cu(2)−O(5′)	1.944(7)
Cu(1)−N(3)	2.033(8)	Cu(2)−N(5)	2.012(8)
Cu(1)−N(4)	1.996(9)	Cu(2)−N(6)	1.995(9)
Cu(1)−N(1)	2.194(9)	Cu(2)−O(2)	2.131(8)
Cu(4)−O(8)	1.995(7)	Cu(3)−O(4′)	1.963(7)
Cu(4)−N(9)	2.040(8)	Cu(3)−O(6)	1.922(8)
Cu(4)−N(10)	1.983(10)	Cu(3)−N(7)	2.013(7)
Cu(4)−N(12)	1.999(9)	Cu(3)−N(8)	1.998(8)
Cu(4)−N(11)	2.222(9)	Cu(3)−O(7)	2.152(8)

[a] Symmetry code: (′) $-x$, $2 - y$, $1 - z$.

carboxylate. The phen nitrogens N(1) and N(11) are located at the apical positions at slightly longer distances. For both the Cu(2) and the Cu(3) atoms, N donors of the chelating phen ligand and two oxygens from the bridging adipate [O(3) and O(5′) for Cu(2) and O(4′) and O(6) for Cu(3)] occupy the basal plane. Oxygen atoms O(2) and O(7) of the bridging carboxylate are located at their respective axial sites (Figure 7). The atoms in the axial O−Cu−Cu−O fragment are considerably bent with ∠O(2)−Cu(2)−Cu(3′) = 168.2(2)° and ∠O(7′)−Cu(3′)−Cu(2) = 149.9(2)°. Correspondingly, the four phen ligands almost normal to the Cu(1)−Cu(2)−Cu(3) axis show intramolecular face-to-face $\pi-\pi$ interactions but in a slightly offset mode. The Cu(2)−Cu(3′) distance is 3.191(2) Å, and metals Cu(1)−Cu(2) and Cu(3)−Cu(4) are separated by 4.486(2) and 4.422(2) Å, respectively. Each adipate bridges four Cu(II) ions; the central Cu(2) and Cu(3) atoms are bridged by three adipate and the other metals are bridged by a single adipate dianion. The two independent crystallographic adipate dianions have different conformations (gauche−anti−gauche and anti−anti−gauche). In the crystal structure, each cationic part is arranged in a plane, and is surrounded by six other cations to form a hexagonal array. Pyridine rings N(1) and N(11), of phenanthroline ligands bound to Cu(1) and Cu(4), respectively, interact with

(29) Zheng, Y.-Q.; Sun, J.; Lin, J.-L. *Z. Anorg. Allg. Chem.* **2000**, *626*, 816.

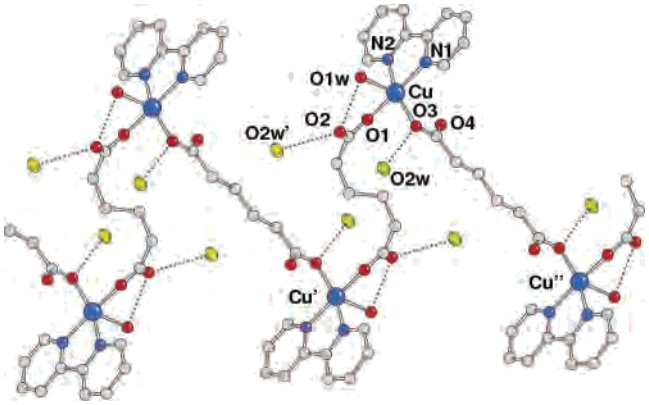

Figure 8. The polymeric chain of **5** [the dotted lines represent H-bonds and the ellipsoids indicate lattice water molecules].

Table 6. Coordination Bond Lengths (Å) for Complexes **5**−**7**

		Complex **5**[a]	
Cu−O(1)	1.929(2)	Cu−O(1w)	2.362(2)
Cu−O(3)	1.981(2)	Cu−Cu′	9.443(2)
Cu−N(1)	2.008(2)	Cu−Cu″	11.639(3)
Cu−N(2)	2.018(2)		
		Complex **6**[b]	
Cu(1)−O(1′)	1.964(4)	Cu(2)−O(2′)	1.955(4)
Cu(1)−O(3)	1.956(5)	Cu(2)−O(4)	1.927(4)
Cu(1)−N(1)	1.997(5)	Cu(2)−N(3)	1.974(5)
Cu(1)−N(2)	1.982(5)	Cu(2)−N(4)	1.983(5)
Cu(1)−O(1w)	2.189(4)	Cu(2)−O(2″)	2.503(5)
Cu(1)−Cu(2)	2.970(1)	Cu(2)−Cu(2‴)	3.378(2)
		Complex **7**[c]	
Cu(1)−O(1)	1.939(4)	Cu(2)−O(3)	1.963(3)
Cu(1)−O(2)	1.964(4)	Cu(2)−O(4)	1.946(4)
Cu(1)−N(1)	1.985(4)	Cu(2)−N(3)	2.008(4)
Cu(1)−N(2)	2.008(5)	Cu(2)−N(4)	2.012(4)
Cu(1)−O(5)	2.263(3)	Cu(2)−O(7)	2.231(3)
Cu(1)−Cu(1′)	3.0070(15)	Cu(2)−Cu(2″)	2.9889(14)

[a] Symmetry codes: (′) $-x, 3-y, -z$; (″) $1-x, 2-y, -z$. [b] Symmetry codes: (′) $1-x, y-1/2, -z+3/2$; (″) $x, -y+1/2, z-1/2$; (‴) $1-x, -y, 1-z$. [c] Symmetry codes: (′) $1-x, y, 1-z$; (″) $2-x, y, -z$.

those of nearby complexes forming aromatic $\pi-\pi$ interactions (Table 4). The unit cell shows a void of 609.9 Å^3, corresponding to 7.1% of its volume, for potential solvent. A mononuclear complex [Cu(phen)$_2$(L$_1$)] with pendent adipate,[30] which can be considered a building block for this octanuclear entity, was reported a few years ago. Its coordination geometry is similar to the copper ion's site located in the Cu_8 complex.

Structure Description of Complex 5. The crystal structure presents Cu(bpy)(H$_2$O) units bridged by adipate dianions with the occurrence of a 1D zigzag coordination polymer (Figure 8). A selection of bond lengths is reported in Table 6. A comparison of coordination distances of the dinuclear complex **1** indicates close, comparable values and is thus not affected by the dimensionality of the complex. The atoms in the basal N_2O_2 plane are tetrahedrally distorted (displacements of ±0.12 Å), and, as a result, the copper ion is displaced by 0.20 Å from this plane toward the apical water ligand. In the chain, the metal ions are coplanar and alternatively separated by 9.443(2) and 11.639(3) Å, with a

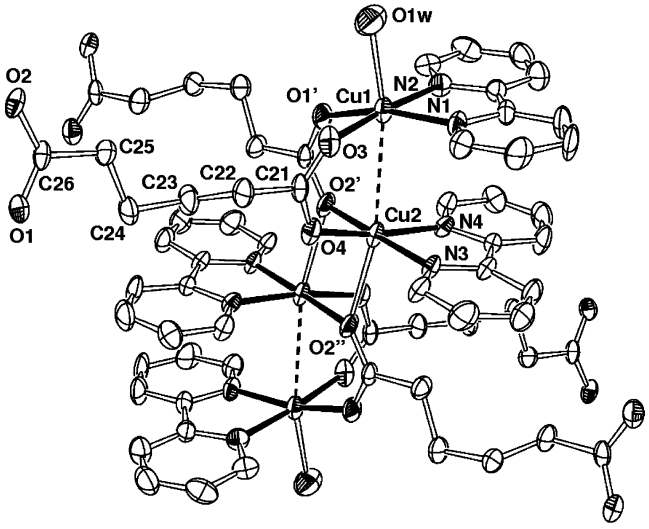

Figure 9. An ORTEP drawing of the tetranuclear building block of **6**.

Cu−Cu−Cu angle of 60.64°. Both independent dicarboxylate dianions that are detected in the cell are arranged about an inversion center. These act as bis-unidentate ligands and adopt a different conformation, which have a gauche−anti−gauche and an anti−anti−anti arrangement, with carbon atoms in the O$_2$C−C−C−C chain that forms dihedral angles of 66.31 and 178.46°, respectively (neglecting the sign). A H-bonding scheme is formed by the aquo ligand O(1w) and the lattice water molecule O(2w), promoting a 2D layer network of the complex (Table S2, Supporting Information). The former makes a strong intramolecular hydrogen bond with the uncoordinated oxygen of adipate [O(1w)−O(2) = 2.700(3) Å] as observed in **4** but also with a symmetry related O(4) oxygen. The lattice water molecule acts as H-donor and bridge adipate oxygens O(3) and O(2) of adjacent chains (Figure 8). Finally, face-to-face aromatic bpy interactions occurring among the nearby chains enhance the dimensionality to 3D. Zheng et al. reported a similar coordination polymer of [Cu(phen)(H$_2$O)] units connected by adipate ligands that behave alternatively as bis-chelating and bis-monodentate,[31] thereby leading to a pseudo octahedral coordination for Cu(II). The metal ions are separated by 9.284 and 9.962 Å, with O$_2$C−C−C−C torsion angles of 59.50 and 124.61° for the centrosymmetric adipate dianions. This topology, when compared with the present structure, seems dictated by the absence of lattice water molecules (rather than by the different N,N-donor ligand) that favors the chelating behavior of carboxylate groups of one adipate.

Structure Description of Complex 6. The crystal structure consists of doubly bridged dimeric Cu(II) units arranged about an inversion center and linked by an oxygen adipate that acts as a bridging donor with a Cu(2)−O(2′)−Cu(2) angle of 97.8(2)°, thus forming tetranuclear units. Figure 9 shows a view of the fundamental structural motif found in the design of the 2D framework that is depicted in Figure 10 with adipate dianions showing a μ_5 coordination mode. The coordination geometry around each copper ion is

(30) Zheng, Y.-Q.; Sun, J.; Lin, J.-L. *Z. Anorg. Allg. Chem.* **2001**, *627*, 90.

(31) Zheng, Y.-Q.; Liu, W.-H.; Lin, J.-L.; Gu, L.-Y. *Z. Anorg. Allg. Chem.* **2002**, *628*, 829.

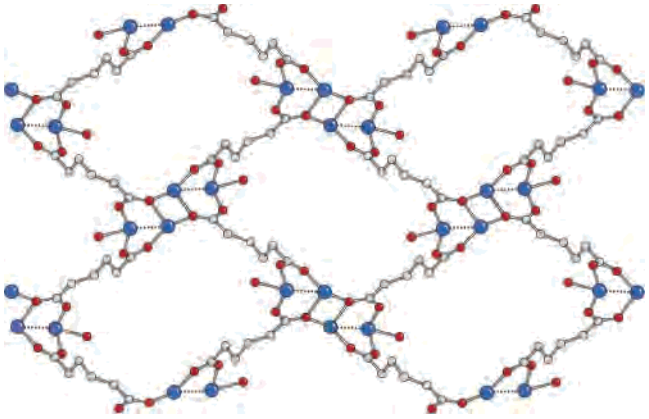

Figure 10. The 2D layered structure of **6** in the [001] direction showing the rhomboid-net (bpy ligands are not shown for clarity).

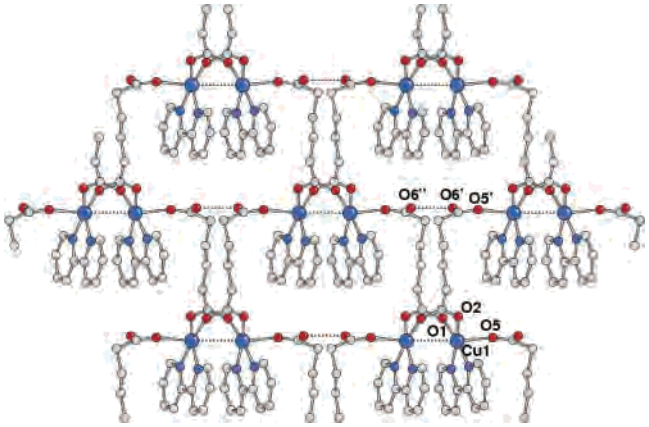

Figure 11. The 2D layered structure of **7** built up by Cu(1) ions. A similar layer is constructed by the other independent copper ion.

approximately square pyramidal with the N donors of chelating bpy and two oxygens of the carboxylate occupying the basal sites. A bridging oxygen O(2) and a water molecule O(1w) are located at the apical positions at slightly longer distances (Table 6). The atoms in the axial O−Cu−Cu−O fragment are not collinear but slightly bent with O(1w)−Cu(1)−Cu(2) and Cu(1)−Cu(2)−O(2″) angles of 164.84(13) and 164.08(9)°, respectively. In each dimeric unit the Cu(1) and Cu(2) metals, separated by 2.970(1) Å, are displaced by about 0.03(1) and 0.33(1) Å toward the apical donor from their respective basal coordination planes, which form a dihedral angle of 21.5(6)°. The adipate dianion adopts a twist conformation (anti−gauche−anti) with torsion angles along the C chain of 175.2(6), 71.7(7), and 177.1(7)°, and terminal carboxyl groups are rotated by 22.3(5)° with respect to one another. Each adipate is coordinated to five metal ions via four oxygen atoms resulting in a corrugated 2D sheet having a rhomboid gridlike topology with dimensions 10.943 × 10.943 Å and developed in the *bc*-plane as shown in Figure 10. The 2D networks, piled in the [100] direction, form small channels that account for a void volume of ca. 718.7 Å^3 (22.2% per unit cell) and are occupied by lattice water molecules and perchlorate anions (Figure S1, Supporting Information). Adjacent layers interlock themselves giving origin to face-to-face bpy interactions, which are responsible for the overall stability of the supramolecular arrangement. The bpy ligand planes form a dihedral angle of 3.56°, while the distance between their centroids is 4.462 Å (Table 4).

Structure Description of Complex 7. The structural analysis evidence indicates that **7** is comprised of dinuclear $[Cu(bpy)]_2^{4+}$ units double bridged by carboxylate groups of adipate anions that act as monodentate ligands with the other carboxylate toward a symmetry related copper ion (Figure 11). Thus each adipate is connected to three metal centers in a μ_3 coordination fashion, with an anti−anti−gauche arrangement of the C atom chain. There are two crystallographic independent metal ions in the asymmetric unit, Cu(1) and Cu(2), that display a square pyramidal coordination geometry with N donors of chelating bpy ligand and two oxygens of the carboxylate occupying the basal sites. At the apex of the pyramid is an oxygen from another carboxylate. A 2-fold axis relates the copper ions of the dimer, and the axial O−Cu−Cu−O fragment is not collinear but slightly bent with an O(5)−Cu(1)−Cu(1′) angle of 169.27(9)° and a value of 162.91(8)° for the corresponding Cu(2). The angles formed by the coordination planes are 21.47(13) and 19.83(13)°, and the dihedral angles formed by the facing bpy ligands are 13.20(9) and 16.04(8)°, respectively for Cu(1) and Cu(2). The latter values indicate that the bpy ligands are slightly divergent with respect to the almost parallel arrangement observed in the copper pairs of **2** and **6**. The Cu−Cu distances inside the dimer, 3.0070(15) and 2.9889(13) Å, are close and comparable for the two crystallographically different copper ions. The $[Cu(bpy)(L_1)]_2$ building blocks, both for Cu(1) and Cu(2), form distinct 2D nets separated by a space, which accounts for ca. 20.3% of the unit cell.[32] Lattice water molecules and BF_4^- counteranions occupy these voids and disrupt the pseudo center of symmetry between the sheets. (Figure S2, Supporting Information). This unprecedented layered structure, with the dimensions 9.399(2) × 9.399(2) Å, is built up in the *ab*-plane (Figure 11) when considering the Cu−Cu midpoints as the nodes of the (4,4) topology network. The small BF_4^- counteranions seem to act as a template for the construction of this unexpected architecture. Because the BF_4^- counteranion plays a vital role in the construction of the 3D architecture, the number of BF_4^- per unit cell is very important.[10a,b] To maintain the neutrality of the complex, one of the dicarboxylates must be formulated as the monoprotonated form during the formation of the self-assembly so as to restrict the number of BF_4^- counteranion per unit cell. A selection of bond lengths is reported in Table 6. The C−O(6) carboxyl bond distance of 1.302(5) Å (Figure 11) and the C−O(8) bond of the other independent adipate, 1.276(5) Å, are indicative of a single bond character. Inside the layer, the symmetry related O(6′) and O(6″) oxygens are separated by 2.439 Å (Figure 11), indicating a strong H-bond, as is also seen in the corresponding layer built by Cu(2) where the OH···O distance is 2.466 Å (Table S3, Supporting Information). These features are consistent with the hypothesis of the protonated carboxylate group, but are likely disordered over the OH−O bridges. A 3D architecture

(32) Spek, A. L. *Acta. Crystallogr. Sect A* **1990**, *46*, C34.

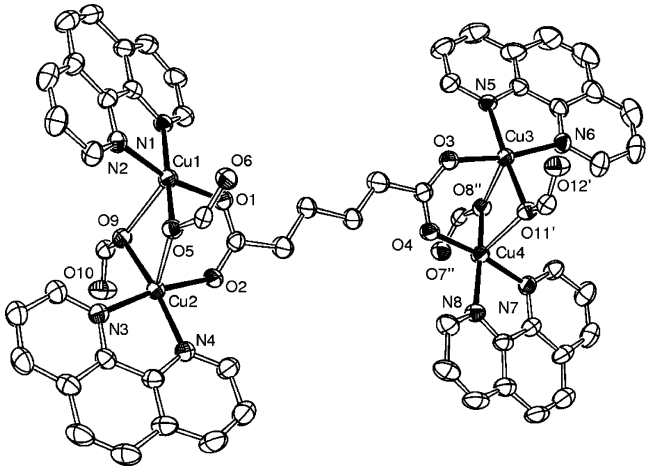

Figure 12. An ORTEP drawing of the metal dimers doubly bridged by two oxygen adipate donors and connected by a bis-bridging adipate in **8**.

Table 7. Coordination Bond Lengths (Å) for Complex **8**[a]

Cu(1)−O(1)	1.948(3)	Cu(3)−O(3)	1.942(4)
Cu(1)−O(5)	1.954(4)	Cu(3)−O(11′)	1.945(4)
Cu(1)−N(1)	2.005(4)	Cu(3)−N(5)	2.000(5)
Cu(1)−N(2)	2.008(4)	Cu(3)−N(6)	2.017(5)
Cu(1)−O(9)	2.319(4)	Cu(3)−O(8″)	2.346(4)
Cu(2)−O(2)	1.934(3)	Cu(4)−O(4)	1.952(3)
Cu(2)−O(9)	1.960(4)	Cu(4)−O(8″)	1.951(4)
Cu(2)−N(3)	2.001(4)	Cu(4)−N(7)	2.007(4)
Cu(2)−N(4)	2.008(5)	Cu(4)−N(8)	2.008(5)
Cu(2)−O(5)	2.259(4)	Cu(4)−O(11′)	2.269(4)
Cu(1)−Cu(2)	3.143(2)	Cu(3)−Cu(4)	3.110(2)

[a] Symmetry code: (′) $x, y-1, z$; (″) $x+1, y, z$.

Table 8. Observed Conformations of the Crystallographic Independent Adipate Anions in Complexes **4**−**8**

4	gauche−anti−gauche	anti−anti−gauche
5	anti−anti-anti	gauche−anti−gauche
6	two anti−gauche−anti	
7	anti−anti−gauche	
8	two anti−anti−anti	one gauche−anti−gauche

is achieved through a H-bonding scheme involving lattice water molecules with carboxylate oxygens and BF_4^- counteranions.

Structure Description of Complex 8. The crystal structure of **8** is composed of dinuclear metal entities showing a configuration different than those reported in the previous complexes (containing dimeric metal units). In this case the metals are double bridged by two oxygen adipate donors and connected by a bis-bridging dicarboxylate (Figure 12). This feature induces the Cu_2 dimers to not show facing phenanthroline ligands. On the basis of these connections, the crystal packing shows 2D layers with a brick-wall architecture (Figure S3, Supporting Information). The four Cu(II) ions in the asymmetric unit have a square pyramidal coordination geometry. The basal plane of each metal (Figure 12) is occupied by chelating phen nitrogens and by two oxygen atoms from adipate dianions. Of the latter donors, one is a bridging oxygen, thus resulting at the apical site of the adjacent metal. The second donor comes from the bis-bridging adipate. The Cu(1)−Cu(2) and Cu(3)−Cu(4) distances are 3.143 (2) and 3.110(2) Å, respectively, indicative of a metal−metal interaction. The Cu−N and Cu−O bond distances (Table 7) average to 2.006(5) and 1.939(4) Å, respectively, and are close and comparable [within their estimated standard deviations (esd's)] to the values reported here for the other structures. On the other hand, the Cu−O apical distances are significantly different inside each dinuclear unit, and they average to 2.333(4) Å for Cu(1)−O(9) and Cu(3)−O(8″) and to 2.264(4) Å for Cu(2) and Cu(4). It is worth noting that the coordination bond angles involving the apical oxygen deviate considerably from ideal values, ranging from 78.16(14) to 109.13(16)°. All of the basal coordination planes have coplanar atoms (±0.05 Å) with copper ions slightly displaced toward the apical oxygen [0.14, 0.10, 0.06, and 0.13 Å for Cu(1)−(4), respectively]. The conformations of the three independent adipate dianions are different: the bis-bridging and one of the bis-unidentate have an extended chain [along the C backbone, the torsion angles, neglecting the sign, are in the ranges 177.1(6)−178.3(6)° and 168.2(5)−179.8(5)°, respectively], and the bis-unidentate adipate is twisted, with torsion angles of −67.3(7), −175.0(5), and 64.9(7)° (gauche−anti−gauche).

Scheme 2

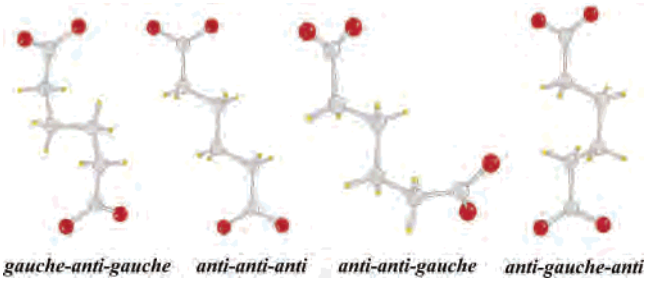

The conformational freedom of the dicarboxylates yields a novel 2D framework with a brick-wall topology having the dimensions 11.165 × 18.812 Å. The voids inside this architecture are filled by perchlorate counteranions that guarantee the electroneutrality of the complex and by a lattice water molecule. The latter molecule is anchored at the framework [O(1w)−O(10) = 2.925 Å] and also forms a weak H-bond with a ClO_4^- oxygen [O(1w)−O = 3.072 Å]. Finally, the structure is stabilized by $\pi-\pi$ interactions occurring between phenanthroline ligands of pillared adjacent layers (Table 4) and leads to a 3D network.

Structural Comparison of Adipate Complexes. All of the complexes containing adipate dianions show metal ions in a square pyramidal coordination sphere with coordination bond lengths and angles falling in a range usually found for analogous copper complexes. More interestingly, the adipate shows a variety of structural motifs due to the different conformations adopted by the adipate carbon aliphatic backbone that allows the construction of high dimensional, porous architectures. The different conformations observed for the crystallographically independent adipate ligands in complexes **4**−**8**, which are summarized in Table 8 and sketched out in Scheme 2, lead to polynuclear Cu(II) coordination complexes of different topology.

As a matter of fact, the different connectivities exhibited by adipate dianions contribute to the delineation of the different dimensionality of the complexes. In fact, adipate dianions exhibit a bis-bridging mode (either syn−syn or

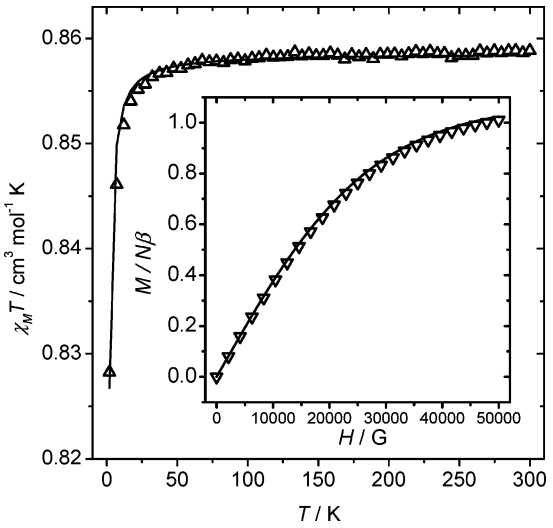

Figure 13. A plot of the $\chi_M T$ vs T for **1**. The solid line indicates the best fit. Shown in the inset is a plot of the reduced magnetization [$M/(N\beta)$] for **1**. The solid line corresponds to Brillouin law.

syn−anti) in **4**, a bis-monodentate coordination fashion in the 1D polymer of **5**, a μ_5 coordination in **6**, a simultaneous bridging and unidentate behavior in **7**, and, finally, the concurrent presence of bis-bridging and bis-monodentate anions in **8.**

Magnetic Study. To make proper magneto-structural correlations, we have divided this section according to the types of bridges that link the copper ions. Out of eight complexes, **1** and **5** only possess the long carboxylate (glutarate/adipate) as a bridging ligand; four of them (**2**, **3**, **6**, and **7**) have two syn−syn carboxylate bridging ligands. Complexes **2** and **3** are tetranuclear Cu_4 systems (vide infra) and complexes **6** and **7** are 2D polymers. Finally, complexes **4** and **8** have syn−syn carboxylate bridging ligands and, simultaneously, other "magnetically significant" bridges (vide supra).

Complexes 1 and 5 (Only Carboxylate as Bridging Ligand). Complex **1** is dinuclear with two glutarate dianions as bridging ligands, and complex **5** is a 1D polymer with only one adipate dianion as a bridging ligand between Cu(II) ions. The magnetic properties of **1** as $\chi_M T$ *vs* T plot (χ_M is the molar magnetic susceptibility for two Cu^{II} ions) with the reduced magnetization ($M/(N\beta)$ *vs* H, inset) are shown in Figure 13. The value of $\chi_M T$ at 300 K is 0.86 cm^3·mol^{-1}·K, which is as expected for two magnetically quasi-isolated spin doublets ($g > 2.00$). Starting from room temperature, $\chi_M T$ values are almost constant up to 50 K, and then they decrease quickly to 0.83 cm^3·mol^{-1}·K at 2 K. This feature is characteristic of weak antiferromagnetic interactions. The reduced molar magnetization at 2 K (Figure 13, inset) clearly corroborates that the antiferromagnetic coupling between the metal ions is very small. The $M/N\beta$ value at 5 T is close to 2.0 $N\beta$ and the curve practically follows the Brillouin function for $g = 2.14$.

Experimental data of the dinuclear Cu(II) entity of **1** have been fitted by applying the Bleaney−Bowers formula[33] and using the Hamiltonian $H = -JS_1S_2$. The best-fit parameters obtained are $J = -0.20 \pm 0.01$ cm^{-1}, $g = 2.14 \pm 0.01$ and $R = 1.6 \times 10^{-6}$, where R is the agreement factor defined as $\sum_i[(\chi_M T)_{obs} - (\chi_M T)_{calc}]^2/\sum_i[(\chi_M T)_{obs}]^2$. Although the Cu−N coordination is short−short (well directed toward the magnetic orbitals, $d_{x^2-y^2}$) the small J value can be interpreted as a consequence of the almost negligible overlap between the Cu(II) ions through the long bridge or it could be attributed to intermolecular interactions between dinuclear units, assuming that the intramolecular J value is zero, because there are five carbon atoms in the bridge skeleton.

For complex **5** the value of $\chi_M T$ at 300 K is 0.44 cm^3·mol^{-1}·K, which is as expected for one magnetically quasi-isolated spin doublet with $g > 2.00$ (Figure S4, Supporting Information). Starting from room temperature, $\chi_M T$ values are almost constant up to 50 K, then decreasing quickly to 0.39 cm^3·mol^{-1}·K at 2 K, which indicates weak antiferromagnetic interactions. The reduced molar magnetization at 2 K (Figure S4, inset) clearly corroborates that the antiferromagnetic coupling is very small. The $M/N\beta$ value at 5 T is close to 1.0 $N\beta$ and the curve practically follows the Brillouin function for $g = 2.15$.

For the 1D Cu(II) entity of **5**, we have fitted the experimental data by applying the formula for an uniform 1D Cu(II) system, as given by Bonner and Fisher.[34] The best-fit parameters obtained are $J = -0.25 \pm 0.01$ cm^{-1}, $g = 2.15 \pm 0.01$, and $R = 2.8 \times 10^{-6}$. Likewise, in the case of **1**, the small J value can be interpreted as a consequence of the almost negligible overlap between the Cu(II) ions through the long bridge or it could be attributed to intermolecular interaction between 1D units by assuming that the intrachain J value is zero, such as in complex **1**.

Complexes 2, 3, and 6 (two syn−syn Carboxylates as Bridging Ligands). For complex **2** the χ_M vs T curve is typical one for an antiferromagnetically coupled dinuclear system (Figure 14A); it shows a maximum at 95 K, and at low temperature there is an increase due to a small percentage of monomeric impurities. The plot of $\chi_M T$ vs T is given in Figure 14B. The value of $\chi_M T$ at 300 K is 0.78 cm^3·mol^{-1}·K, which is as expected for two magnetically quasi-isolated spin doublets ($g > 2.00$). Starting from room temperature $\chi_M T$ values decrease quickly and approach 0 cm^3·mol^{-1}·K at 2 K (with a plateau from 20 K to 2 K), which indicates strong antiferromagnetic interactions.

By assuming that the magnetic interaction through the long carboxylate bridge is nil, we have fitted the magnetic data as a dinuclear one with the Bleaney−Bowers[33] equation and considering the Hamiltonian $H = -JS_1S_2$. The best-fit parameters obtained are $J = -84.1 \pm 0.8$ cm^{-1}, $g = 2.22 \pm 0.01$, ρ (monomeric impurities) = 1.8%, and $R = 5.0 \times 10^{-6}$.

The magnetic property of **3** (Figure S5, Supporting Information) is almost the same as that of **2** and by applying the same method, the best-fit parameters obtained are as

(33) Bleaney, B.; Bowers, K. D. *Proc. R. Soc. London Ser. A* **1952**, *214*, 451.
(34) Bonner, J. C.; Fisher, M. E. *Phys. Rev. A* **1964**, *135*, 640.

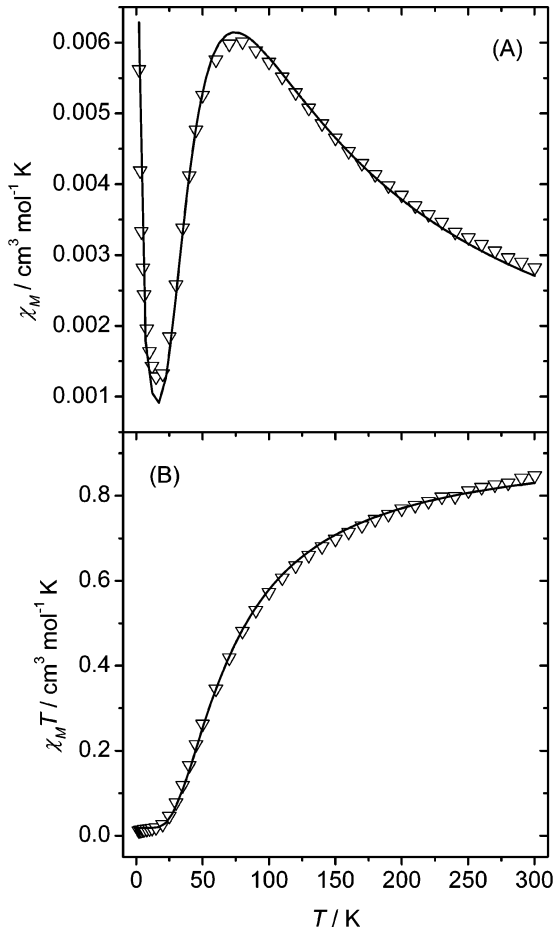

Figure 14. (A) A plot of the χ_M vs T for **2** is shown; (B) plot of the $\chi_M T$ vs T for **2** (the solid line indicates the best fit).

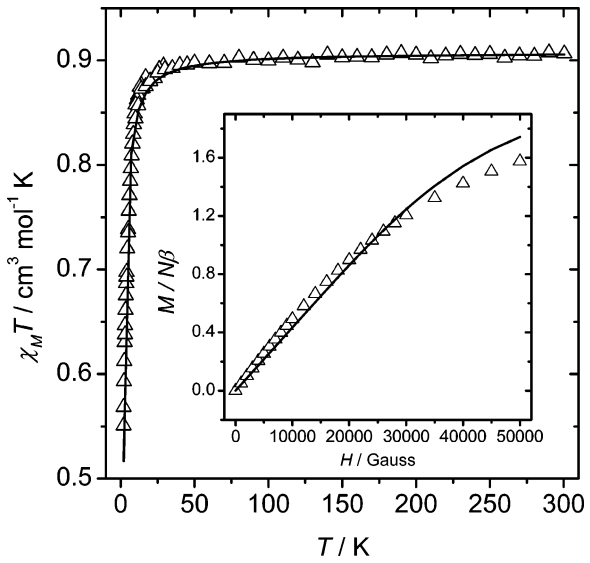

Figure 15. A plot of the $\chi_M T$ vs T for **6** (the solid line indicates the best fit). Shown in the inset is a plot of the reduced magnetization [$M/(N\beta)$] for **6**. The solid line corresponds to Brillouin law.

follows: $J = -81.2 \pm 0.6$ cm^{-1}, $g = 2.15 \pm 0.01$, $\rho = 1.8\%$, and $R = 1.5 \times 10^{-6}$ for **3**.

For complex **6** the value of $\chi_M T$ at 300 K is 0.90 cm^3·mol^{-1}·K, which is the expected value for two isolated Cu(II) ions with g > 2.00 (Figure 15). From room temperature to 50 K, the $\chi_M T$ values are almost constant, and after that, from 50 K to 2 K there is a rapid decrease up to 0.55 cm^3·mol^{-1}·K indicating small antiferromagnetic coupling between Cu^{II} ions. The curve of the reduced magnetization for two Cu(II) (inset of Figure 15) indicates no saturation value is achieved at 5T (almost 1.7 $N\beta$, instead of 2 $N\beta$ for two noncoupled ions).

As described in the crystallographic portion, complex **6** is a complicated network formed by dimeric Cu_2 entities linked by a long dicarboxylate ligand. Thus, we have fitted the magnetic data of **6** by considering a dinuclear entity (assuming a negligible magnetic interaction through the long dicarboxylate) by the Hamiltonian $H = -JS_1S_2$, and by applying the formula of Bleaney−Bowers.[33] The best-fit parameters are provided as follows: $J = -1.93 \pm 0.02$ cm^{-1}, $g = 2.20 \pm 0.02$, and $R = 2.1 \times 10^{-4}$. This J value indicates that the coupling between the Cu(II) centers is weakly antiferromagnetic. Anyway, from a theoretical point of view, there is another possible magnetic pathway through Cu2 and Cu2″ ions by means of a short−long (equatorial−axial) syn−anti carboxylate coordination mode, which in some cases operates by weak ferromagnetic interactions. This feature could be important to interpret the weak J value. Unfortunately, all attempts to either apply the molecular field approach for finding a possible J' value between dinuclear entities or by assuming directly two J values in the tetranuclear entity were unsuccessful and did not improve the results.

Apparently, the structural data of complexes **2**, **3**, and **6** are very similar, but the J value is significantly different for **6**. For interpreting this feature, we have to carefully consider the structure of the dinuclear entities in these three complexes.

General Aspects on the Magnetic Properties of the syn−syn Carboxylate Bridging Ligands. The versatility of carboxylate as a ligand is illustrated by the variety of its coordination modes while acting as a bridge,[35−38] the most common being the so-called syn−syn, syn−anti, and anti−anti modes. Focusing on the former coordination mode in Cu(II) complexes, there is a marked dependence of J on the number of carboxylate bridges (4 > 3 > 2 > 1).[39−42] The J parameter may have a high value for $n = 4$ ($J > 300$ cm^{-1}),[33,40,43,44] whereas there is only one very distorted complex reported in the literature when $n = 3$ ($J = -40.7$

(35) Deacon, G. B.; Phillips, R. J. *Coord. Chem. Rev.* **1980**, *33*, 227.
(36) Melnik, M. *Coord. Chem. Rev.***1981**, *36*, 1.
(37) Kato, M.; Muto, Y. *Coord. Chem. Rev.* **1988**, *92*, 45.
(38) C. Oldham, C. In *Comprehensive Coordination Chemistry*; Wilkinson, G., Gillard, R. D., McCleverty, J.A., Eds.; Pergamon Press: Oxford, 1987; Vol. 2, p 435.
(39) Figgis, B. N.; Martin, R. L. *J. Chem. Soc.* **1956**, 3837.
(40) (a) Tokii, T.; Emori, S.; Muto, Y. *Bull. Chem. Soc. Jpn.* **1974**, *47*, 2887. (b) Mikuriya, M.; Kida, S.; Ueda, I.; Tokii, T.; Muto, Y. *Bull. Chem. Soc. Jpn.* **1977**, *50*, 2464.
(41) Madalan, A. M.; Paraschiv, C.; Sutter, J.-P.; Schmidtmann, M.; Muller, A.; Andruh, M. *Cryst. Growth Des.* **2005**, *5*, 707.
(42) Psomas, G.; Raptopoulou, C. P.; Iordanidis, L.; Samara, C. D.; Tangoulis, V.; Kessissoglou, D. P. *Inorg. Chem.* **2000**, *39*, 3042.
(43) Doedens, R. J. *Prog. Inorg. Chem.* **1990**, *38*, 97.
(44) Rodríguez-Fortea, A.; Alemany, P.; Alvarez, S.; Ruiz, E. *Chem. Eur. J.* **2001**, *7*, 627.

Scheme 3

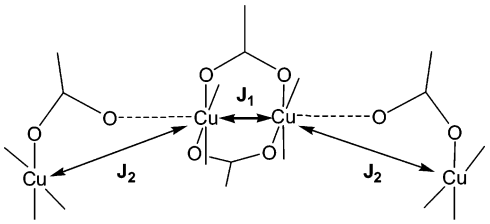

cm^{-1}).[45] For $n = 2$, such as in complexes **2**, **3**, and **6**, the structural motif $\{Cu_2(\mu\text{-carboxylate-O,O}')_2\}$ has been encountered in several dinuclear and 1D Cu(II) complexes.[16a,40−42,46,47] Finally, with only one carboxylate bridging group in syn−syn geometry, two similar complexes have been reported: $[\{LCuX\}_2(\mu\text{-benzoate})](ClO_4)$ (X = Cl, Br; L = 1,4,7-trimethyl-1,4,7-triazacyclononane).[48] The *J* values are very small: −1.2 and −2.3 cm^{-1}, respectively.

Focusing our interest in the complexes with two carboxylate bridging groups we realize that the *J* values reported vary from ca. −100 to ca. −7 cm^{-1}, and it is very difficult to rationalize such a wide range. Undoubtedly, here the Cu−Cu distance and the τ(Addison) parameter[49] (very important for the overlap between the magnetic orbitals) play a crucial role. In **6** the coupling is, surprisingly, much smaller and is likely due to the distortion in the dihedral angle formed by moving the carboxylate ligands (16.5 and 12.2°) together to the noticeable τ parameter (0.19 and 0.13), far from the ideal square pyramidal geometry (the best overlap and the greater antiferromagnetic coupling). Indeed, as postulated through theoretical calculation by Rodríguez-Fortea et al.,[44] deviations of the regular geometry of these syn−syn carboxylate ligands always have an effect that results in a reduction of the antiferromagnetic coupling. Lastly, it may be assumed that there are other unknown factors responsible for reducing the *J* value in **6** in such a noticeable way. Thus, further complexes with two bridging carboxylate ligands and other substituents are required to furnish an assessment of this issue.

Complexes 4 and 8 (syn−syn Carboxylates + Other Significant Bridging Ligands). In **4**, inside the octanuclear complex, two Cu_4 entities are connected by adipate bridges, and these four copper atoms are linked by two carboxylate bridges in apical−equatorial syn−anti coordination mode (between the terminal and the central copper ions) and two that are in equatorial−equatorial syn−syn coordination modes (between the two central copper ions).

In a first approach, the magnetic pathway through the long adipate bridge can be considered as negligible. The very small influence of these bridges will be noticeable only at very low temperature. Thus, from a magnetic point of view, we can draw a scheme (Scheme 3) showing the two central syn−syn carboxylate bridges and the two syn−anti terminal ones beside the two main *J* parameters (J_1 and J_2). From a geometrical point of view, the two J_2 values will be slightly different.

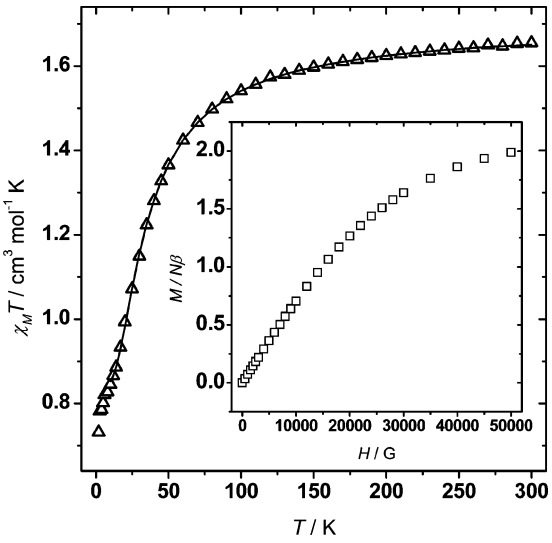

Figure 16. A plot of the $\chi_M T$ vs *T* for **4** (the solid line indicates the best fit). Shown in the inset is a plot of the reduced magnetization [$M/(N\beta)$] for **4**.

For complex **4** the value of $\chi_M T$ at 300 K is 1.62 $cm^3 \cdot mol^{-1} \cdot K$, which is as expected for four magnetically quasi-isolated spin doublets with $g > 2.00$ (Figure 16). Starting from room temperature, $\chi_M T$ values monotonously decrease to 0.70 $cm^3 \cdot mol^{-1} \cdot K$ at 2 K with a pronounced variation in the slope of the curve between 20 K and 2 K. This feature is characteristic of global antiferromagnetic interactions. The reduced molar magnetization ($M/N\beta$) at 2 K (Figure 16, inset) is close to 2.0 $N\beta$ and follows the Brillouin law.

The fitting of the magnetic susceptibility data has been carried out by a full-diagonalization method, applying the Clumag program.[50] To avoid the difficulty due to the change of the slope at low temperatures (likely due to the intermolecular interactions through the adipate ligands), the experimental data below 10 K were removed from the fit. Thus the best-fit parameters obtained are $J_1 = -41.0 \pm 0.5$ cm^{-1}, $J_2 = -2.6 \pm 0.5 cm^{-1}$, $g = 2.13 \pm 0.01$, and $R = 3.1 \times 10^{-5}$. J_1 value agrees with those previously found and are comparable to those reported in the literature for similar double syn−syn carboxylate bridges. Concerning J_2, the structure shows an apical−equatorial coordination mode of carboxylate in syn−anti fashion that currently gives small antiferromagnetic coupling depending on the distortion of the square pyramidal geometry of the copper atoms (in this case, the two central atoms). For complex **4** this distortion, with regard to the ideal square pyramidal geometry, is almost zero ($\tau = 0.07$ and 0, respectively), and is responsible for the noticeable reduction in the *J* value. However, the two

(45) Geetha, K.; Chakravarty, A. R. *J. Chem. Soc. Dalton Trans*. **1999**, 1623.
(46) Tokii, T.; Watanabe, N.; Nakashima, M.; Muto, Y.; Morooka, M.; Ohba, S.; Satto, Y. *Bull. Chem. Soc. Jpn.* **1990**, *63*, 364.
(47) Mishima, N.; Matsuo, C.; Koikawa, M.; Tokii, T. *Mol. Cryst. Liq. Cryst.* **2002**, *376*, 359.
(48) Bürger, K.-S.; Chaudhuri, P.; Wieghardt, K. *Inorg. Chem.* **1996**, *35*, 2704.
(49) Addison, A. W.; Rao, T. N.; Reedjik, J.; van Rijn, J.; Verschoor, C. G. *J. Chem. Soc. Dalton Trans.* **1984**, 1349.
(50) The series of calculations was made using the computer program CLUMAG, which uses the irreducible tensor operator (ITO) formalism: Gatteschi, D. Pardi, L. *Gazz. Chim. Ital*. **1993**, *123*, 23.

Scheme 4

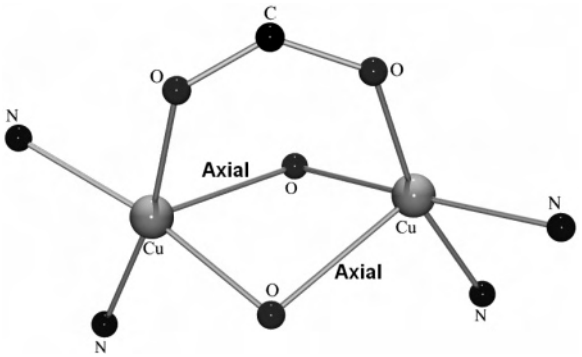

Cu−O (apical) distances are very short for this type of coordination (2.144 and 2.129 Å). These two features (negligible τ and short Cu−Cu distance) may clarify the experimental J_2 value of -2.6 cm^{-1}. The different values of J_1 and J_2 explain the reduced magnetization that tends toward 2 $N\beta$ at 5 T. The two central copper atoms are strongly antiferromagnetically coupled, which at low temperature give a $N\beta$ value of 0. However, the other two terminal copper ions are quasi isolated and at 5 T the $N\beta$ value is, thus, that which corresponds to these two ions.

For **8** the value of $\chi_M T$ at 300 K is 0.84 cm^3·mol^{-1}·K, which is as expected for two magnetically quasi-isolated spin doublets with $g > 2.00$ (Figure S6, Supporting Information). Starting from room temperature, $\chi_M T$ values decrease smoothly up to 50 K, and then they decrease quickly to 0.05 cm^3·mol^{-1}·K at 2 K indicating antiferromagnetic interactions. The reduced molar magnetization at 2 K (Figure S6, inset) corroborates that this antiferromagnetic coupling is noticeable. The $M/N\beta$ value at 5 T is close to 0.22 $N\beta$ instead of 2 $N\beta$ (for two Cu(II) ions) and the curve does not follow the Brillouin law.

Actually, **8** is a peculiar 2D system in which two different dinuclear entities are linked in different ways by the long adipate ligands. Thus, from a magnetic point of view, it can be considered as a dinuclear Cu(II) entity. The fit of the susceptibility data has been carried out by applying the Bleaney−Bowers formula,[33] and the best-fit parameters obtained are $J = -9.2 \pm 0.1$ cm^{-1}, $g = 2.16 \pm 0.01$, and $R = 6.7 \times 10^{-4}$. The relatively small J value can be interpreted as a consequence of the structure of the dinuclear entity (Scheme 4). Although there are two nonequivalent dinuclear entities, their structural parameters (distances and angles) are close and comparable so that we can consider only one.To simplify the calculation. From Scheme 4 we can clearly realize that there are three different magnetic pathways: two Cu−O−Cu bridges in apical−equatorial coordination mode and one syn−syn carboxylate bridge in equatorial−equatorial bridging fashion. The four Cu(II) ions are almost square planar (τ parameters are 0.086 and 0 for one entity and 0.10 and 0.08 for the second entity).

As a result of the equatorial−axial coordination mode in the two Cu−O−Cu bridges, the overlap between the two Cu(II) ions through the oxo bridges will be very weak, resulting in a very small J value. The non-negligible experimental J value is also due to the syn−syn equatorial−equatorial coordination of the carboxylate bridge. The small J values found in this case have been stated above while dealing with the generalities of the syn−syn carboxylate bridges.

Complex 7. As stated in the structural part, complex **7** is composed of dinuclear units double bridged by carboxylate groups and adipate dianions that act as monodentate ligands. Owing to the presence of the two carboxylate syn−syn groups, an antiferromagnetic coupling between the two Cu(II) ions must be operative. Assuming all other interactions as almost negligible, the $\chi_M T$ value must tend toward 0 cm^3·mol^{-1}·K when the temperature is lowered to 2 K. However, the shape of the $\chi_M T$ curve is unexpected (Figure S7, Supporting Information). The starting value at room temperature is as expected (0.8 cm^3·mol^{-1}·K) but it is impossible to explain the plateau relative to the structure. Furthermore, the reduced magnetization [$M/(N\beta)$] tends toward 0.9 $N\beta$, which is a very high value when considering any noticeable AF coupling. The magnetic measurements were carried out twice each on two different set of samples and the results were found to be identical. It is necessary to state that the purity of the powder sample has also been verified with the X-ray powder pattern, which matches very well with the simulated powder pattern of single-crystal X-ray data (Figure S8, Supporting Information).

Conclusion

The present study reveals that the structural diversity in Cu(II)−glutarate/adipate systems is achieved by conformational freedom of the dicarboxylate backbone as well as by the type of counteranion, H-bonding, and $\pi-\pi$ stacking interactions between the N,N-donor chelating ligands. As the adipate dianion is more flexible than the glutarate one, we have obtained 1D and 2D coordination polymers rather than oligonuclear complexes. With the adipate dianion we have successfully synthesized an octanuclear complex, which is structurally similar to that which was previously reported by us using succinate dianion. However, an analogous octanuclear complex could not be synthesized using the glutarate dianion. Thus the design of an octanuclear species is made feasible by the conformational freedom of the carbon aliphatic chain of the adipate dianion, as compared to that of succinate. Moreover the carbon backbone of adipate presents a greater conformational freedom, and it seems to also be responsible for the generation of voids, where lattice water molecules and perchlorate/tetrafluroborate counteranions get stabilized through H-bonding. The dimensionality is also directed by the chelating bpy/phen ligands used, because these ancillary ligands inhibit two metal coordination sites, thus reducing the expansion of coordination polymers. With the exception of a discrete dinuclear complex, all of the complexes exhibit copper dimeric fragments with intermetallic distances of ca. ~3.0 Å, which is indicative of a possible metal−metal interaction. The magnetic studies reveal antiferromagenteic interactions between the metal centers for all of the complexes.

Acknowledgment. The authors acknowledge the Seed Support for young teachers under the Potential for Excellence Scheme of Jadavpur University (DG), Grant BQU2003-00539 of the Spanish Government (JR) and Council of Scientific and Industrial Research, New Delhi (NRC).

Supporting Information Available: Crystallographic data in CIF format for the structures reported. Tables of H-bonds distances (for complexes **1**, **5**, and **7**) along with some additional figures. This material is available free of charge via the Internet at http://pubs.acs.org.

IC061720V